PERSPECTIVE

Check for updates

Soft matter physics of the ground beneath our feet

Anne Voigtländer, [ID] †*[az] Morgane Houssais, [ID] †*[b] Karol A. Bacik, [ID] [c] Ian C. Bourg, [ID] [d] Justin C. Burton, [ID] [e] Karen E. Daniels, [ID] [f] Sujit S. Datta, [ID] [g] Emanuela Del Gado, [ID] [h] Nakul S. Deshpande, [ID] [f] Olivier Devauchelle, [ID] [i] Behrooz Ferdowsi, [ID] [j] Rachel Glade, [ID] [k] Lucas Goehring, [ID] [l] Ian J. Hewitt, [ID] [m] Douglas Jerolmack, [ID] [n] Ruben Juanes, [ID] [o] Arshad Kudrolli, [ID] [b] Ching-Yao Lai, [ID] [p] Wei Li, [ID] [oy] Claire Masteller, [ID] [q] Kavinda Nissanka, [ID] [e] Allan M. Rubin, [ID] [r] Howard A. Stone, [ID] *[s] Jenny Suckale, [ID] [t] Nathalie M. Vriend, [ID] [u] John S. Wettlaufer [ID] [vw] and Judy Q. Yang [ID] [x]

The soft part of the Earth's surface – the ground beneath our feet – constitutes the basis for life and natural resources, yet a general physical understanding of the ground is still lacking. In this critical time of climate change, cross-pollination of scientific approaches is urgently needed to better understand the behavior of our planet's surface. The major topics in current research in this area cross different disciplines, spanning geosciences, and various aspects of engineering, material sciences, physics, chemistry, and biology. Among these, soft matter physics has emerged as a fundamental nexus connecting and underpinning many research questions. This perspective article is a multi-voice effort to bring together different views and approaches, questions and insights, from researchers that work in this emerging area, the soft matter physics of the ground beneath our feet. In particular, we identify four major challenges concerned with the dynamics in and of the ground: (I) modeling from the grain scale, (II) near-criticality, (III) bridging scales, and (IV) life. For each challenge, we present a selection of topics by individual authors, providing specific context, recent advances, and open questions. Through this, we seek to provide an overview of the opportunities for the broad Soft Matter community to contribute to the fundamental understanding of the physics of the ground, strive towards a common language, and encourage new collaborations across the broad spectrum of scientists interested in the matter of the Earth's surface.

[a] *German Research Centre for Geosciences (GFZ), Geomorphology, Telegrafenberg, 14473 Potsdam, Germany. E-mail: avoigtlaender@lbl.gov*

[b] *Department of Physics, Clark University, 950 Main St, Worcester, MA 01610, USA*

[c] *Department of Mathematics, Massachusetts Institute of Technology, 77 Massachusetts Avenue, Cambridge, MA 02139, USA*

[d] *Civil and Environmental Engineering (CEE) and High Meadows Environmental Institute (HMEI), Princeton University, E208 EQuad, Princeton, NJ 08540, USA*

[e] *Department of Physics, Emory University, 400 Dowman Dr, Atlanta, GA 30033, USA*

[f] *North Carolina State University, 2401 Stinson Dr, Raleigh, NC 27607, USA*

[g] *Department of Chemical and Biological Engineering, Princeton University, Princeton, NJ 08544, USA*

[h] *Department of Physics, Institute for Soft Matter Synthesis and Metrology, Georgetown University, Washington, DC, USA*

[i] *Institut de Physique du Globe de Paris, Université Paris Cité, 1 rue Jussieu, CNRS, F-75005 Paris, France*

[j] *Department of Civil and Environmental Engineering, jUniversity of Houston, Houston, TX 77204, USA*

[k] *Earth & Environmental Sciences Department and Mechanical Engineering Department, University of Rochester, 227 Hutchison Hall, P.O. Box 270221, Rochester, NY 14627, USA*

[l] *School of Science and Technology, Nottingham Trent University, Nottingham NG11 8NS, UK*

[m] *Mathematical Institute, University of Oxford, Woodstock Road, Oxford OX2 6GG, UK*

[n] *Department of Earth & Environmental Science, University of Pennsylvania, Philadelphia, PA 19104, USA*

[o] *Department of Civil and Environmental Engineering, Massachusetts Institute of Technology, 77 Massachusetts Avenue, Cambridge, MA 02139, USA*

[p] *Department of Geophysics, Stanford University, Stanford, CA 94305, USA*

[q] *Department of Earth and Planetary Sciences, Washington University in St. Louis, St. Louis, MO, USA*

[r] *Department of Geosciences, Princeton University, Princeton, NJ 08544, USA*

[s] *Department of Mechanical and Aerospace Engineering, Princeton University, Princeton, NJ 08544, USA*

[t] *Computational and Mathematical Engineering, and Environmental Engineering, Stanford University, Stanford, CA 94305, USA*

[u] *Department of Mechanical Engineering, University of Colorado at Boulder, Boulder, CO 80309, USA*

[v] *Departments of Earth & Planetary Sciences, Mathematics and Physics, Yale University, New Haven, CT 06520, USA*

[w] *Nordic Institute for Theoretical Physics, 106 91, Stockholm, Sweden*

[x] *Saint Anthony Falls Laboratory and Department of Civil, Environmental, and Geo-Engineering, University of Minnesota, Minneapolis, MN, USA*

[y] *Stony Brook University, Department of Civil Engineering, Stony Brook, NY 11794, USA*

[z] *Lawrence Berkeley National Laboratory (LBNL), Energy Geosciences Division, 1 Cyclotron Rd, Berkeley, CA 94720, USA*

† These authors contributed equally to this work. The following authors are in alphabetical order.

The ground beneath our feet, plain and static as it might seem, holds the key to many pressing global issues. More than ever, in a world that is experiencing global warming and changing precipitation patterns, we need to better understand, predict, and feasibly control processes within the ground that can cause natural hazards,[1] shape future landscapes,[2–5] impact the health of our agricultural lands,[6] and sequester carbon.[7]

What we are calling the ground is all the complex material at the surface of the Earth that is not essentially a single-phase natural fluid, such as air and water. It is either a composite solid (*e.g.*, crystalline or sedimentary rocks, or ice, of various compositions, age, and deformation history) or – and most commonly – an assembly of grains of different types (*e.g.*, sand grains, clay platelets, shells, ice crystals, boulders, bacteria). The ground evolves because it is constantly being processed by reactive solutions, biological activity, capillary and thermal stresses, and sheared by gravitational forces and fluid flows. As a result, locally and at a given time t, the ground exhibits normal and shear strains $\gamma(t)$, an effective solid – or packing – fraction $\phi(t)$, and associated porosity $s(t) = 1 - \phi(t)$ occupied by a volume fraction $w(t)$ of an effective liquid, most often natural water. Over time, w can vary from 0% (dry) to 100% (fully saturated, and sometimes overflowing), through intermediate values (partially saturated). Studies of the physical and chemical dynamics of such a system – coarsely, a heterogeneous and fragile "sponge" or pile of sticky grains – give rise to a multitude of Soft Matter problems.

Echoing the richness of the ground, a multitude of disciplines investigate the thin layer making the Earth's surface, including the Earth, environmental, and material sciences, engineering, physics, chemistry, and biology. Different disciplines tend to have different cultures and approaches, as well as different motivations, constraints, and even notations. As a result, a wide and complementary range of foci regarding temporal and spatial scales, concepts, laboratory, and field study methods coexist. Nevertheless, opportunities for scientific exchanges between these different communities which study processes happening at Earth's surface remain rare. This article is a perspective on the key-concepts and main challenges one faces in and out of well-controlled experiments and models of the ground (Fig. 1). Through specific examples, it also attempts to present some of the fantastic messiness one is confronted with, and enriched by, while studying the natural environment. Once clarified what are the mechanics of various systems over different length and time scales, field site location and conditions, process interactions and feedbacks, the fundamental questions at the heart of the discussion are: how can the complexity of natures dynamics and mechanics be simplified, measured, down-scaled, and structured to fit into a model, or are such simplifications impossible? How can the development of complex material rheology frameworks be of future use? How do we treat intermittency in natural phenomena? What are the expressions of near-criticality in nature, and over what scales should we consider it?

Our intention here is to be both broad and specific. Broad in the sense of the conceptual framework outlined, and what we consider as soft matter (Fig. 1). Specific in highlighting some of the ongoing fronts of the scientific research and techniques on the ground beneath our feet, to inspire future, new and collaborative works. The effort was initiated by a workshop organized by the princeton center for theoretical science (PCTS) in January 2022, where the authors discussed recent results from their individual field of expertise. These contributions, enriched by the authors' collective conversation and efforts, turned into this article. Albeit their heterogeneity, they share similar broad challenges concerning concepts and scales, technical and methodological issues. The specific sub-sections represent only a small fraction of the many outstanding questions related to the field of "physics of the ground", nevertheless they allow to present how this is an emerging research area where fundamental soft matter questions come together with interdisciplinary problems and impact. With this perspective paper we want to highlight this new research direction for soft matter by sharing examples of specific efforts and results recently obtained on such fronts.

The paper is organized into four sections, corresponding to four major scientific challenges we have identified as what is mainly ahead of us to model the ground (Fig. 1). These challenges are integral to the field of soft matter, yet they also have unique aspects when one studies the natural environment.

I – The challenge of modeling from the grain scale.

The ground is essentially a range of partially-wet particulate (hence porous) systems where chemical, physical, and biological processes occur (see magenta box in Fig. 1). Modeling each of these processes from the smaller scale is both fundamental and essential to building larger-scale and multi-parameter, multi-physics models.

II – The challenge of near-criticality.

The Earth surface constantly evolves and sets itself near its material yield criterion (typically, a critical shear stress σ_c). As a result, we mainly live in and observe a quasi-static environment – an apparently stable ground – but which is often about to fail (Fig. 1c and d). Surveying and predicting the ground's mechanical behavior, in particular the rare times it deforms plastically (*e.g.*, during floods and landslides), requires good understanding and modeling of its near-critical behavior. This challenge demands advancements in both fundamental physics and development of new methods of quantitative observations.

III – The challenge of bridging scales.

All Earth (near-)surface processes occur at given length and time scales. Some mechanisms are universal across a wide range of spatial and temporal scales, some structures are hierarchical and emergent, some material properties are bounded with typical magnitudes, lengths, and characteristic times or rates. Knowledge of how and when to bridge scales, mathematically, numerically, and methodologically from the laboratory to the field sites (and *vice versa*) is a difficult key to forge (dark blue arrow on Fig. 1), but one unlocks advanced predictive capabilities.

IV – The challenge(s) of life.

Living matter has the unique property of reproducing itself, and growing or decaying over time. The self-propelled motion
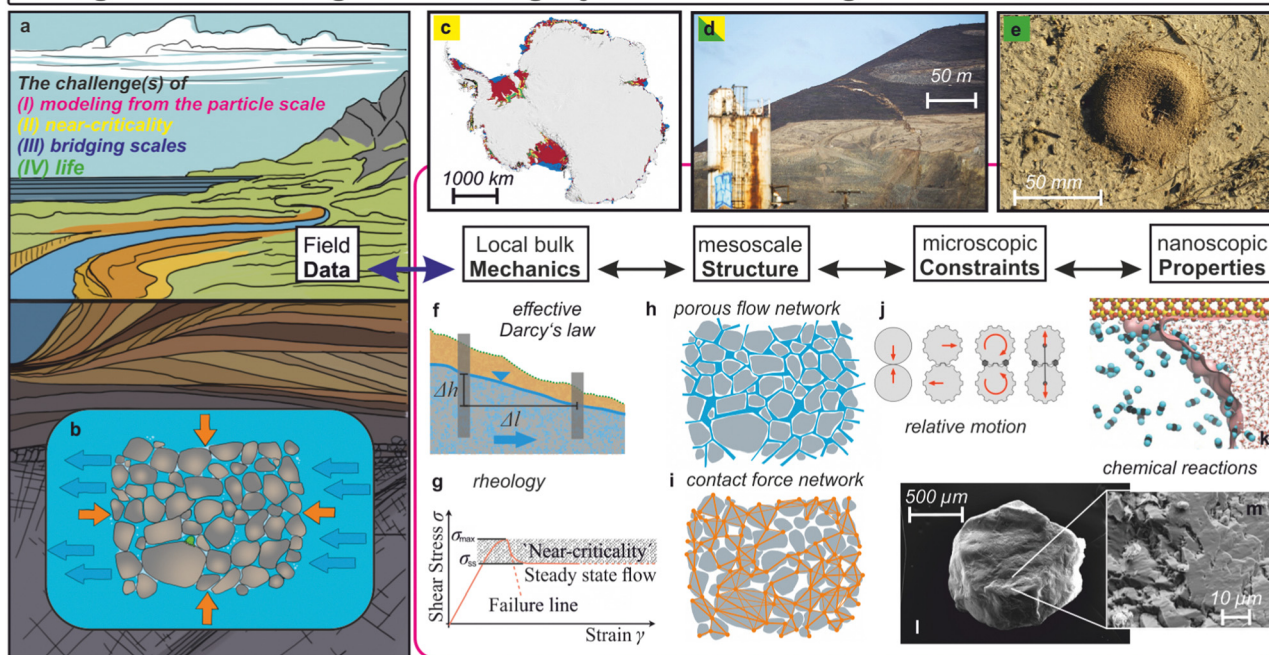
Fig. 1 (a) Overview sketch of the four challenges of modeling the soft matter physics of the ground identified in this paper: (I) modeling processes from the grain scale; (II) measuring and capturing the ground dynamics near critical states; (III) connecting laboratory and theory results to field-scale observations; (IV) understanding and taking into account the many effects of life. (b) In a given element of the ground, subjected to normal stresses (orange arrows) and a mean groundwater flow (blue arrows), the soft matter physics of the ground encompasses simultaneously multiple phases, processes, dimensions, and scales, which can have various expressions at the Earth's surface, *e.g.*, (c) an Antarctica map showing ice-shelf areas vulnerable to hydro-fracture (marked in red) in a warming world by Lai *et al.*;[8] (d) a photograph of a crack that appeared on Jan 3 2018 in Rattlesnake Ridge, near Union Gap, WA, April 2018 (200 km from the 2014 Oso landslide with industrial infrastructure in the foreground, Photo credit: Shawn Gust, Yakima Herald-Republic *via* AP); and (e) a photograph of a mound of grains built by ants (imaggeo/EGU). To model the multi-dynamics of the ground, diverse methods, concepts, and approaches are used to link the ground's properties, constraints, structures, mechanics, and observational data. For example, models of (f) effective groundwater flow, or (g) rheological behavior in experiments and simulations, rely on assumptions relative to (h) porous flow and (i) contact force networks. (j) Individual motions in these networks are constrained by the properties and mechanisms of the phases involved.[9] Often a phase can both be a constituent of the bulk system and define an interface where chemical reactions occur, *e.g.*, (k) a CO_2 bubble in contact with a water meniscus in a silica nanopore (courtesy of I.C. Bourg). As a result of these interactions, for example, a mineral particle such as a natural quartz sand grain (l) can display a chemo-mechanically altered surface topography (m), as seen in the scanning electron microscopy images (courtesy of A. Voigtländer). Such nanoscale phenomena can in turn affect the effective rheology of the ground and groundwater flow.

of many organisms is another specific impact of life on the environment. Many organisms contribute to the constant alteration of their surroundings, while also depending on it (Fig. 1d and e). The interconnections between all forms of life – including human life – and the dynamics of the ground, although obeying the laws of physics, bring additional complexity and carry a large number of original and pressing questions.

Within each one of these four main challenges (section), each contribution (sub-section) present a specific topic: its specific context, some recent advances, and open questions. These sub-sections are only a selection of topics, which illustrate through specific problems the four main challenges.

1 The challenge of modeling from the grain scale

Efforts to understand the dynamics of the ground from the scale of a single grain inform our definitions of transients,

steady state dynamics (*e.g.*, rheology), fundamental causes for instability growth, and the interactions between different physical processes. Fundamentally, these efforts aim to identify, visualize or parameterize, and quantify the relevant elementary phenomena happening at the grain scale. This section presents a few examples of ongoing efforts in this domain based on experimental, numerical, and analytical approaches (Fig. 1).

In particular, Sections 1.1 and 1.2 illustrate advances by considering Earth materials, such as fault gouge or soils, as granular assemblages, eventually impacted by pore fluid pressure. Section 1.3 highlights how *in situ* observations are generating new insight on flow, transport, and mechanics in these heterogeneous porous materials. Section 1.4 discusses Eulerian computational approaches that can capture the complex deformation of ductile, cohesive Earth materials (such as erosion or desiccation cracking). Finally, Section 1.5 highlights how grain–fluid interactions can add significant complexity to grain scale processes, for example in situations where solid surfaces impact the stability of interfacial liquid water films.

1.1 The role of granular flow in fault friction – A. M. Rubin & B. Ferdowsi

Context. Many phenomena associated with the physics of the ground can be viewed as manifestations of granular flows. For example, field observations indicate that faults in the Earth are invariably filled with granular material (gouge) derived from wear of the surrounding rock.[10,11] At depth, these fault gouges are infiltrated by water, with important implications for thermal pressurization at high slip speeds.[12,13] But important aspects of the rheology of even nominally dry gouge are poorly understood. Laboratory experiments have long established that at sliding speeds low enough for inertial and thermal effects to be unimportant, variations in friction (the ratio of shear to normal stress during sliding) for both rock and gouge are typically only a few percent of the nominal friction value of around 0.6–0.8, over sliding speeds or strain rates that span orders of magnitude.[11] Despite their small magnitude, these variations in friction are responsible for, among other things, whether faults slide stably at the plate tectonic rate of centimeters per year, or slip episodically in damaging earthquakes at rates of meters per second.[14]

Numerical models of fault slip require a constitutive law for fault friction. The current state-of-the-art, originally conceived for two rough surfaces in contact but observed to apply to sheared gouge layers as well, falls under the heading of "rate- and state-dependent" friction. In this formalism, friction depends upon the fault sliding rate (or strain rate), and a more nebulous property termed "state".[14] State is conventionally thought to reflect a combination of the true contact area and the intrinsic strength of those contacts.[15] Also conventionally, the state dependence is thought to be due to time-dependent plastic flow or chemical bonding at those contacts, although the opaque nature of rock makes the origin of state evolution difficult to decipher.[16] How state evolves for surfaces not at steady-state sliding is parameterized by "state evolution laws" that are largely empirical, yet still do not adequately describe all the relevant features of laboratory experiments.[17]

Numerical simulations of faults obeying rate-state friction show that the precise description of state evolution significantly influences processes of interest to Earth scientists (*e.g.*, earthquake nucleation[18]). The lack of an accurate or physics-based description of state evolution thus severely hampers our ability to extrapolate the results of numerical models of fault slip to the Earth.

Recent advances. Recent discrete element method (DEM) simulations of a granular gouge layer show that much of the phenomenology of transient rock and gouge friction seen in laboratory experiments (both the rate-dependence and the state-dependence) can be reproduced by numerical models in which this dependence arises only from momentum transfer between the grains, with no chemical reactions or time-dependent plasticity at grain/grain contacts.[19] Panel (a) of Fig. 2 shows a snapshot from a DEM simulation designed to mimic laboratory rock friction experiments. A 2D layer, periodic in the x and y directions, is sheared between two rigid parallel plates. A specified velocity history in the x direction is applied to a very stiff spring attached to the upper plate, while a constant normal stress of 5 MPa is maintained in the z direction. A constant sliding friction acts at grain/grain contacts. Panel (b) shows the friction signal, relative to the future steady-state value, following simulated velocity steps of ±1 or 2 orders of magnitude. At the time of the velocity step, there is an abrupt change in stress of the same sign as that of the step (the "direct velocity effect" of rate-state friction), followed by an exponential decay to a new steady-state value (the "state evolution effect"). The magnitudes of the direct and evolution effects are approximately proportional to the logarithm of the velocity jump, with an e-folding strain for friction evolution of ∼0.13.

These results are similar to those from laboratory friction experiments on rock and many other materials. The solid black lines in Fig. 2c indicate the friction signals, relative to the prior steady state value, following velocity steps of ±1 or 2 orders of magnitude from experiments on synthetic quartz gouge.[17] The magnitude of the logarithmic rate- and state-dependence in the DEM and lab experiments are similar to within a factor of ∼2 (there is some rounding and diminishing of the peaks in panel (c) not present in panel (b) because the elastic stiffness of the lab system is smaller). The red lines in Fig. 2c are a fit to the data using the empirical "slip" version of the rate-state friction equations,[11,14,17] using a single set of parameter values for all 4 steps.

Open questions. The source of the rate- and state-dependence in the DEM, which lacks time-dependence at the contact scale, remains an area of active investigation. It appears possible to understand the direct strain-rate dependence semi-quantitatively in terms of an Arrhenius process, with the kinetic energy of the grains playing the role of the molecular kinetic energy in the classical understanding of rate-state friction,[20] as grains hop from one potential well to another.[19] Although the nature of granular friction has been studied extensively in the physics and engineering literature, most of this work concerns friction during steady flow.[21–27] The transient frictional properties of granular flow thus represent a rich and underexplored field of interest to Earth scientists, physicists, and engineers.

1.2 Force chains underpin emergent poromechanical behavior in granular media – W. Li & R. Juanes

Context. In addition to granular flows, another foundation of our ability to model the dynamics of the ground is our understanding of poromechanics, *i.e.*, the manner in which pore fluids influence granular mechanics. In this context, photoelasticity has a long history as a technique to quantify internal stresses in solid bodies,[28] but it has been traditionally applied to granular media consisting of cylindrical (usually circular) disks.[29,30] This particle geometry has the advantage of allowing for precise quantification of stresses,[31] but the disadvantage that it prevents connectivity within the pore space, thus restricting severely its purpose as an analogue of permeable porous media, where fluid flow and mechanical deformation are often strongly coupled.[32] This is because it is effective stress – the fraction of the total stress that is transmitted through the solid skeleton – that controls the
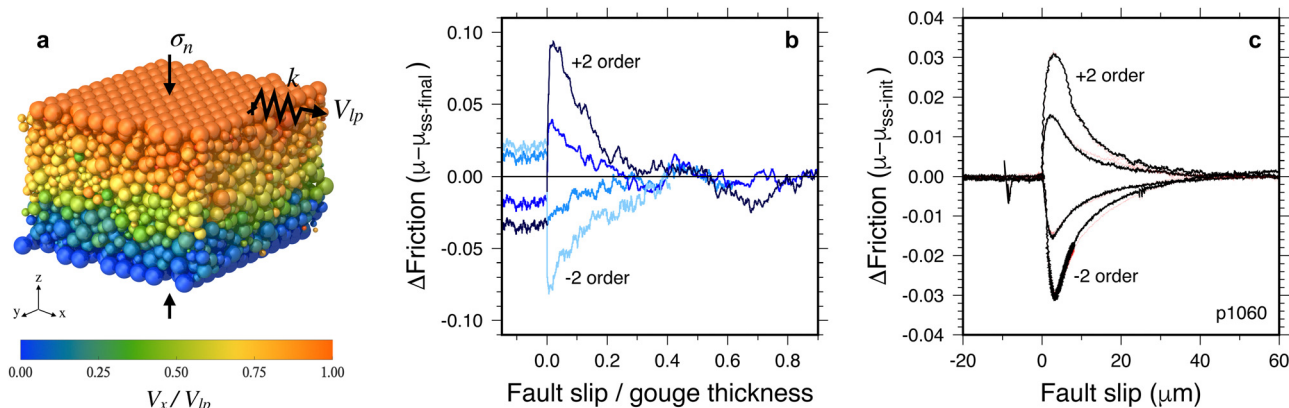
Fig. 2 (a) Snapshot from a DEM simulation of a sheared granular layer.[19] Grains are spherical, polydisperse, and have elastic properties appropriate for glass beads. Colors indicate grain velocity in the x direction, relative to the load-point velocity, averaged over an upper-plate sliding displacement of 1 mean grain diameter. (b) The friction signal, relative to the future steady-state value, following simulated velocity steps of ±1 or 2 orders of magnitude from an initial velocity of 0.01 m s^{-1}.[19] Slip distance is defined to be zero at the time of the step. (c) Solid black lines indicate the friction signals, relative to the prior steady-state value, following velocity steps of ±1 or 2 orders of magnitude at sliding speeds from 1 to 100 μs^{-1}, from experiments conducted in the Penn State Rock and Sediment Mechanics Lab.[17] The starting material is a 3-mm-thick layer of synthetic quartz gouge, with particles ranging from 50–150 μm in diameter (shear ultimately localizes to a narrower zone where particles have been comminuted, a process not modeled in the DEM). The synthetic quartz gouge is nearly steady-state velocity neutral, whereas the DEM is steady-state velocity strengthening. The red lines are a fit to the data using the empirical "Slip" version of the rate-state friction equations ("direct effect" coefficient a = 0.0073; "state evolution effect" coefficient b = 0.0075; e-folding slip distance D_c = 12.2 μm).

mechanical behavior of porous media, from land subsidence due to groundwater pumping to the cohesion of sand in sandcastles.[33] Karl von Terzaghi, father of soil mechanics, introduced the concept of effective stress a century ago.[34,35] Until recently, however, this physical quantity could only be calculated by subtracting pore pressure from the normal total stress, or inferred from its "effect", typically the solid skeleton deformation.

Recent advances. For a proper analogy of a porous medium in terms of pore geometry, connectivity and morphology, a pack of three-dimensional (3D) particles, such as spheres, should be used. Extending photoelasticity to such systems, however, requires developing a method to manufacture residual-stress-free photoelastic particles, and obtaining quantitative information on the forces acting on these 3D particles. A fabrication process similar to "squeeze casting" was recently demonstrated to produce millimeter-scale residual-stress-free photoelastic particles (spheres and other shapes, such as icosahedra) with high geometric accuracy (Fig. 3a and b). The combined photoelastic response from light intensity and light color permits a rough quantification of forces acting on the particles over a wide range of forces. A first application of the new technique, coined photoporomechanics,[36] revealed the evolution of effective stress during vertical consolidation (Fig. 3c and d). In this process, the stresses caused by a sudden load on a fluid-filled granular pack are gradually transmitted through emergent force chains as the fluid drains and excess pore pressure dissipates. The resulting particle–particle force networks originate at the top boundary (where the pore fluid seeps out) and propagate downwards through the pack as the pore pressure gradually dissipates (Fig. 3e).

Open questions. The extension of photoelasticity to 3D particles provides a powerful experimental model system to study the strong coupling of solid and fluid in granular media that take place in geoscience processes like landslides,[37] gas vents from ocean sediments,[38] and injection-induced seismicity.[39] This is especially attractive in three dimensions, where – while long-standing issues related to the interpretation of light transmission in fully-3D stress fields[40] still need to be resolved – the method can form the basis for force-chain tomography.[41]

1.3 *In situ* visualization of soft matter dynamics in granular and porous media – S. S. Datta

Context. In many ways, experimental advancements drive our ability to better model Earth processes by visualizing grain-scale fluid and particle dynamics. In particular, techniques from physical chemistry and colloidal science, coupled with developments in microscopy and imaging science, have yielded unprecedented ability to visualize the dynamics of soft materials in models of complex and crowded environments akin to the porous soils, sediments, aquifers, and reservoirs in the ground beneath our feet. In these cases, the environment alters the material, the material alters the environment, and these coupled dynamics give rise to behaviors that challenge current understanding.

For example, despite its importance in geophysics and in a wide variety of natural and engineered processes,[42–77] prediction and control of complex fluid flow, particle transport, and solid mechanics in porous media is challenging and often operates by trial and error. Even basic prediction of where injected fluid distributes through a porous medium, and of the associated macroscopic resistance to flow, remains elusive due
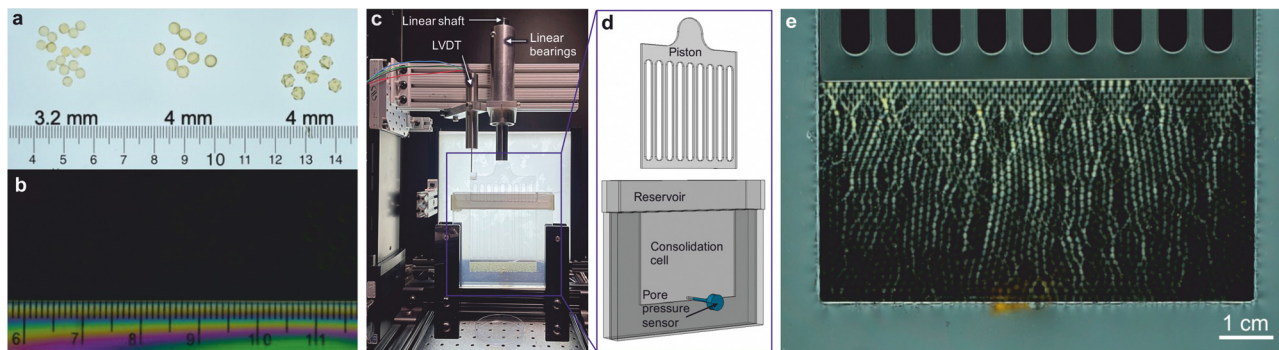
Fig. 3 Consolidation test using photoporomechanics. (a) Millimeter-size photoelastic particles in two different shapes (spheres and icosahedra) under white light. (b) Photoelastic particles under a circular polariscope. The polystyrene ruler, having residual stress, shows color stripes. The particles, being residual-stress-free, are hardly visible.[36] (c) Experimental setup for the 1D consolidation experiment. A granular pack of fluid-saturated photoelastic spheres is loaded suddenly with a constant weight, while the video, deformation, and excess pore pressure are recorded. (d) Detailed schematic of the consolidation cell. Two glass plates are glued with a 2 mm thick U-shaped spacer where the beads are inserted to form a monolayer pack. The excess pore pressure is measured at the bottom of the cell with a pressure sensor. The pore fluid fills the cell to provide a constant-pressure boundary condition. A piston made of a 1.8 mm acrylic plate (with slots cut out to reduce resistance to fluid flow) allows the fluid to seep out of the cell.[36] (e) Snapshot of the photoelastic response of the granular pack during a consolidation test. The force chains – which quantify the Terzaghi stress in the granular pack – develop from the top boundary, then progress downwards through the pack as the pore–fluid pressure diffuses upwards.

to the time-dependent and multi-scale nature of the associated phenomena. Disentangling these interactions through *in situ* visualization is an exciting research frontier. While even basic characterization has traditionally been difficult due to the opacity and complexity of most three-dimensional (3D) environments, confocal microscopy of refractive index-matched fluids and model solid media now enables researchers to directly visualize soft matter dynamics in 3D porous media with controlled pore structures and chemistries.[78]

Recent advances. A common feature of the advances in visualization is the ability to simultaneously probe pore space topology, dynamic changes in fluid microstructure, multi-scale flow patterns, and macroscopic transport, which provides a way to directly connect phenomena across scales. One notable advance is that direct visualizations of flow in 2D and 3D porous media can increasingly capture the structural and chemical heterogeneities of many naturally-occurring media, such as pore size gradients, strata with different permeabilities, and regions of differing surface chemistry.[79–82] Such heterogeneities fundamentally alter fluid displacement pathways and dynamics. In particular, a pore size or surface energy gradient can either suppress or exacerbate both capillary fingering[83] and viscous fingering,[84] distinct interfacial instabilities that typically arise in homogeneous media. Furthermore, for the case of stratified media, visualizations reveal that immiscible fluid displacement is spatially heterogeneous, with different strata being invaded at different rates,[85] leading to differing amounts of fluid removal – phenomena that are not predicted by typically-used spatially-averaged models of fluid flow, but are captured by new theoretical models inspired by the experiments.[86]

A second example is the phenomenon whereby as colloidal particles navigate a porous medium, they can alter the medium by depositing onto (or eroding from) its solid matrix, making prediction of macroscopic particle distributions challenging.[87–103]

Advances in direct visualization have enabled identification of the fundamental mechanisms by which particles are distributed throughout a porous medium, demonstrating that the interplay between hydrodynamic and colloidal interaction forces controls this process.[104] These advances also have enabled characterization of how interactions between particles and trapped non-aqueous fluids influence subsequent transport (Fig. 4a).[105] These results help shed light on the multi-scale interactions between fluids, particles, and porous media that have traditionally been represented in black-box models using "lumped" empirical parameters – guiding the development of more accurate and generalizable models that could be applied in diverse geophysical settings and beyond, for example, in the complex flow behavior of polymer solutions.[106–111]

A third illustration is the use of *in situ* visualizations of hydrogels, *i.e.*, elastic networks of hydrophilic polymers that can absorb large quantities of water, as models of shrinkable granular media, *e.g.*, soft clay-rich soils whose deformations influence the integrity of built structures and barriers for waste isolation.[115–117] Deforming such a soft porous material alters fluid transport through its pores, which in turn further deforms the material. Direct visualization of this coupling between fluid transport and solid deformations has shown how material physicochemical properties that regulate fluid permeability and mechanical deformations, as well as interactions with external boundaries, together control how these materials swell, shrink and deform,[112] fracture,[118] and potentially even self-heal[112] (Fig. 4b) – providing new insights into the desiccation of soft earth materials.

Finally, the development of "transparent soils" using, *e.g.*, granular hydrogels has helped shed light on the behavior of bacteria in 3D granular media over length scales ranging from the single-cell to the community scale[119] (Fig. 4c–e). This capability has revealed that understanding of bacterial motility – which is based on studies performed in bulk
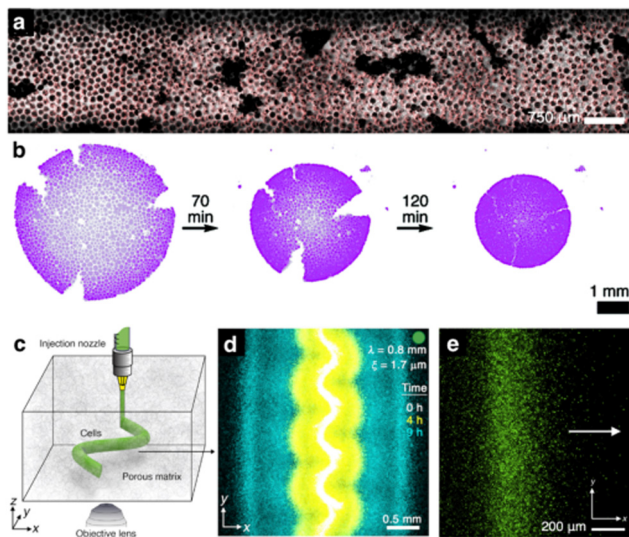
Fig. 4 Illustrations of the capability for *in situ* visualization of soft matter dynamics in granular and porous media. (a) Large-scale confocal micrograph taken inside a 3D porous medium (section through solid matrix shown by black circles), showing trapped oil (additional black) and deposited colloidal particles (red) in the pore space.[105] (b) Self-healing of a cracked packing of hydrogel beads; color shows fluorescence due to an excited dye that has diffused within the hydrogel beads, with an intensity that increases with bead shrinkage.[112] (c) Schematic showing 3D printing of bacteria inside a porous granular hydrogel matrix. (d) Superimposed experimental confocal micrographs (different colors show different times) of bacteria spreading collectively from a 3D-printed population with an undulatory initial structure; the spreading cells smooth out these morphological perturbations. (λ) and (ξ) refer to the undulation wavelength and hydrogel matrix mean pore size, respectively.[113] (e) Magnified view of a front of bacteria spreading by chemotaxis in a crowded, porous, granular hydrogel matrix.[114]

liquid – was incomplete: for example, confinement in a crowded medium fundamentally alters how bacteria move, both at the single cell[120] and population scales,[114] in previously unknown ways. Ultimately, these results could guide the development of new theoretical models[121] to more accurately predict the motion and growth of bacterial populations in complex environments akin to those in the ground beneath our feet, potentially helping to provide quantitative guidelines for the control of these dynamics in processes ranging from bioremediation to agriculture.

Open questions. The examples listed above highlight the utility of direct visualization of soft matter dynamics in model porous media in shedding new light on problems in soft matter of the ground. Moving forward, it will be important for researchers to continue to develop new imaging approaches to access, *e.g.*, 3D fluid flow fields. In addition, a useful direction for future research will be to examine dynamics in granular and porous media with additional complexities such as deformability and rearrangements of the granular matrix and different grain shapes, sizes, surface chemistries, and packing geometries. While a great deal of empirical evidence indicates that these factors strongly alter dynamics in complex environments, unifying principles that describe how remain

lacking. 3D fluid flow observations could provide a way to investigate such principles. This future research work would deepen fundamental understanding of soft matter dynamics in geoscientific settings. Finally, the development of rigorous guidelines for the application in the field of existing soft materials and complex fluids, as well as principles for the formulation of new materials and fluids, remains largely undone. 3D fluid flow observations in porous media could help build such guidelines, and enable researchers in *e.g.*, controlling solute transport and transport-limited chemical reactions in environmental remediation, as well as other industrial and environmental processes.

1.4 Coupled flow and mechanics of clays and muds – I. C. Bourg

Context. Although parts of the ground can be viewed as assemblages of relatively coarse grains (on the order of micrometers or more), other parts hold a significant abundance of fine grained materials with dimensions on the order of nanometers. These materials, collectively referred to as clays or muds, consist of mixtures of inorganic and/or organic solids, particularly clay minerals, nanocrystalline metal oxides, natural organic matter, and biofilms.[122,123] Despite their variable composition, they exhibit common properties including low permeability, cohesion, and strong couplings between mechanics, hydraulics, and pore fluid chemistry[122,124,125] that emerge as particle dimensions approach the length scales (Ångström to tens of nanometers) associated with London dispersion, Debye screening, and orientational correlations in liquid water.

An important aspect of the complex properties of clays and muds is that they can transition from cohesive to non-cohesive and from solid- to liquid-like mechanics depending on conditions, with important implications in efforts to predict phenomena such as fault slip, debris flow, and sediment transport (Sections 1.1, 2.2 and 2.4). A challenge in understanding these properties from the grain scale is that they are inherently multiphysics: whereas interparticle interactions in coarse grained materials predominantly consist of repulsive grain contact forces, potentially supplemented by attraction due to capillary fluid menisci,[126] interparticle interactions in clayey materials involve a variety of attractive and repulsive interactions across thin water films, such as osmotic, electrostatic, van der Waals, hydration, and configurational entropy effects. All these interactions generally have different length scales and sensitivities to particle shape, surface charge, and solution chemistry to take into account.[127,128]

Recent advances. The utility of soft matter physics concepts in simulations of the coupled hydraulic-mechanical-chemical properties of muds is illustrated by a recently-developed "Darcy-Brinkman-Biot" framework.[124] This framework combines the well-established Darcy-Brinkman representation of fluid flow in porous systems with two characteristic lengths scales (*e.g.*, a microporous clay matrix coexisting with a macroscopic flow channel)[129] with representations of the ductile deformation and swelling–shrinking of clay using a chemistry-dependent poromechanics model (captured within

a Terzaghi stress tensor[130]) and a viscoplastic rheology model.[131] Results show that this framework can represent key emergent properties of clays including swelling and shrinking as a function of salinity (Fig. 5a),[124] desiccation cracking during drying (Fig. 5b),[132] and erosion under fast fluid flow (Fig. 5c)[133] on scales relevant to Earth surface dynamics (Fig. 5d).[134]

Open questions. A significant remaining challenge is that the presence of clays or muds creates a vast scale separation between the coarse grain scale – associated with sand grains, grain contacts, force chains, and microbial processes with characteristic scales on the order of 10^{-6} to 10^{-4} m – and the scale of clay colloidal interactions, on the order of 10^{-9} to 10^{-7} m. With the exception of idealized subsurface materials such as pure homogeneous sand or clay, the ground is inherently a multiscale material because of the ubiquitous co-existence of clay or mud with coarser-grained material and/or larger-scales features (e.g., cracks), with more than three orders of magnitude separation in length scale.[124,138,139] Accurate prediction of phenomena such as sediment erosion and debris flows may require combining discrete representations of force chains

between coarse materials with a continuum representation of fluids and a ductile clay matrix.[140,141]

Another important challenge is that the Eulerian treatment of clays illustrated in Fig. 5 requires constitutive relations reflecting the microscale material properties of clay (e.g., rheology, swelling pressure, permeability) as a function of saturation, salinity, compaction, and clay composition (i.e., the relative abundance of different clay minerals or biopolymers). These constitutive relations remain incompletely known, because of the complexity associated with the irregular shapes and the strong impact of interfacial fluids on interparticle interactions between nanometer scale clay colloids and/or biopolymers.[128,138,142,143]

1.5 Nonequilibrium statistical physics of inclusions in ice – J. S. Wettlaufer

Context. Another illustration of the multiphysics couplings that emerge from nanoscale interactions across thin water films is the existence of a layer of liquid water on the surface of ice, even at temperatures well below freezing. These unfrozen films can influence everything from the slipperiness of glaciers to the electrification of thunderclouds.[144]

In cold climates, roads are salted in winter harnessing the freezing point depression of impurities. Each salt crystal, however, abuts an ice surface where the phase change occurs. Less commonly thought of, but equally important, are other mechanisms that can extend the equilibrium domain of a liquid phase into the solid region of the normal phase diagram. The causes of this "premelting", which, in addition to impurities,[145] include surface melting, interface curvature and substrate disorder, allow for the persistence of water at interfaces well below the bulk melting point. The thickness of the liquid film depends on the temperature, soluble impurities, the material properties underlying intermolecular forces, and geometry. A temperature gradient is accompanied by a thermomolecular pressure gradient that drives the unfrozen interfacial liquid from high to low temperatures and hence particles in ice, as shown in Fig. 6, migrate from low to high temperatures. Such premelting dynamics are operative in a wide range of settings, from the heaving of frozen ground and planetary regolith, to the scavenging of atmospheric trace gases by snow and the redistribution of climate proxies in ice sheets, to the collisional processes in protoplanetary disks. Moreover, the unfrozen films act both as a refuge for biota and a transport mechanism for nutrients, waste and the biota themselves.

Recent advances. New research considers such processes in the framework of active matter, wherein particles are endowed with intrinsic mobility mimicking life, and addresses the interplay between a wide range of problems, from extremophiles of both terrestrial and exobiological relevance to ecological dynamics in Earth's cryosphere. For example, biota are found in glaciers, ice sheets, and permafrost, evolving in a complex mobile environment facilitated or hindered by a range of bulk and surface interactions. Survival strategies, such as producing exopolymeric substances and antifreeze glycoproteins, that enhance the interfacial water also facilitate bio-mobility. Such
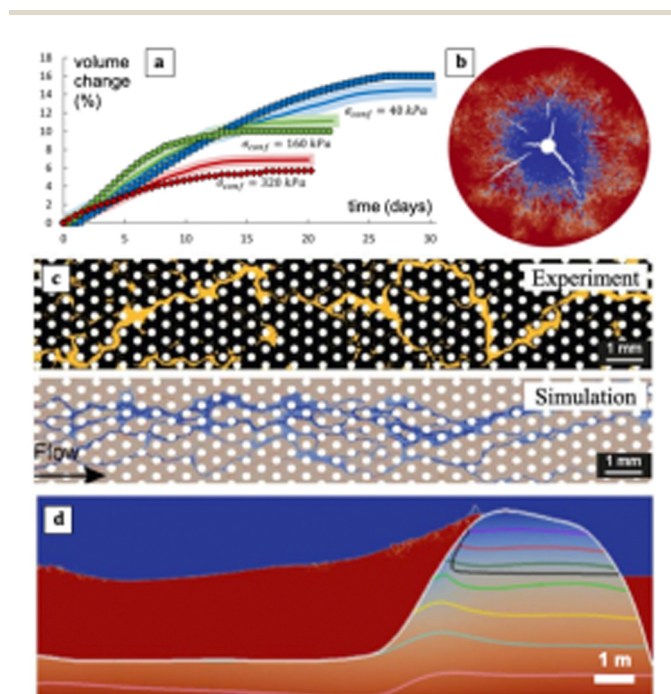

Fig. 5 Darcy-Brinkman-Biot (DBB) simulation of clay: (a) expansion of a clay plug caused by a salinity decrease in a water reservoir in contact with the clay (symbols: measurements at different confining stresses;[135] lines, model predictions[124]). (b) Cracking of a clayey medium in a Hele–Shaw cell upon injection of a non-wetting fluid from the center (red: water-saturated clay, blue: dry clay, white: cracks). Model predictions[132] are qualitatively consistent with experimental observations.[136,137] (c) Experiments and simulations showing flow channelization during biofilm growth in a microfluidic device (channels and biofilm matrix in yellow/black in the experiments, blue/tan in the simulations). The simulations correctly predict the emergence of flow intermittency and channelization associated with intermittent erosion.[133] (d) Wave impact on a poroelastic barrier illustrating the coupling of multiphase flow and Earth surface mechanics on scales of tens of meters (colored lines show von Mises stresses within the barrier).[134]
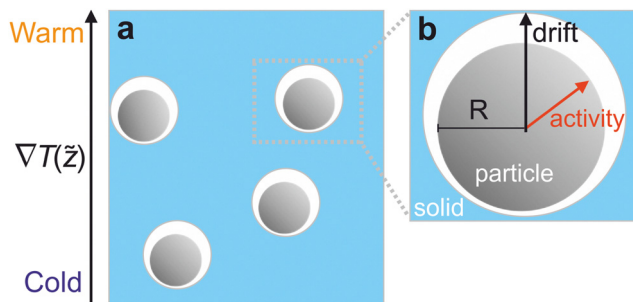
Fig. 6 The interface between ice and inert or living particles is separated by what is called a premelted water film below the bulk melting point. (a) Perspective view of few active particles embedded inside ice against which they premelt and experience an external temperature gradient ∇T, which creates a thermomolecular pressure gradient driving the flow of liquid from high to low temperatures, so that particles translate from low to high temperatures. (b) An expanded view of one active particle inside the solid. The radius of the particle is R, the black arrow shows the drift velocity induced by the temperature gradient, and the red arrow denotes the activity given by an active force (from Vachier and Wettlaufer[146]).

phenomena can be cast in the stochastic framework of active Ornstein–Uhlenbeck dynamics and chemotaxis,[146] to find that for an attractive (repulsive) nutrient source, that thermomolecular motion is enhanced (suppressed) by biolocomotion. This phenomenon is essential for understanding the persistence of life at low temperatures.

Open questions. There are a host of open questions that occupy the attention of soft matter scientists. A vexing problem concerns the relative importance of the deformability of single particles *versus* a matrix of particles. For example, when individual particles are rigid, premelting dynamics will redistribute particles at a freezing front, which itself impacts the local permeability. However, if an individual particle is highly deformable, that deformation may dominate the local permeability. These differences may control the overall stresses in the medium, which recent methods may be able to measure.[147,148] On the biological side, some important questions are (i) how much interfacial water is necessary to sustain life; (ii) how effective are bio-polymers in maintaining this water; (iii) are the polarization forces responsible for the interfacial water deleterious to biota or have they evolved to tolerate them? Clearly, the interaction between these outstanding physical and biological questions has implications for both terrestrial and extraterrestrial environments.

2 The challenge of near-criticality

Traditionally, the field of geophysics has been mainly subdivided between two areas: solid Earth geophysics—concerned with the application of solid mechanics to measuring and modeling rocks and ice over a variety of length and time scales[149,150]—and geophysical fluid dynamics – deeply rooted in applied mathematics and its application to atmospheric and ocean dynamics. Yet, many of the materials in the Earth's critical zone transit between many regimes: athermal to thermal (large to small particles), chemically inert to reactive (sand

to clay), dense to dilute, jammed to creeping to catastrophic (submarine) avalanches and sand storms; and *vice versa via* deposition and lithification. There can be sharp spatial or temporal gradients between these regimes, and often these regimes are mixed with repeated transitions between them. The topics highlighted in this section consider near-critical behaviors in the "soft Earth" regime,[151] which cannot be addressed by fluid or solid mechanics alone.

The study of near-critical behavior in soft materials has a long history and encompasses problems such as the glass transition and deformation, shear-thickening behavior of suspensions, particulate material jamming, solid creep, and fracture dynamics. Most of these systems exhibit behaviors that are non-linear functions (*e.g.*, Fig. 1) of the system's temperature, applied stresses, and density of grains or atoms. Material failure in the environment shares these common features and presents specific challenges. The Earth surface, just as any soft condensed matter near one of their failure criteria, is generally far from equilibrium and nonisotropic. Finding insightful measurements of such system responses, and how to use them practically to predict material failure, has been a crucial scientific endeavor. Section 2.1 presents recent experimental results on this front and their implications for further developing failure prediction in the environment. Different types of environments exhibit near-critical behavior, and they have been recorded and analyzed in different ways: for example, Section 2.2 covers the failure of hillslopes, Section 2.3 presents a recent highly-resolved spatial and temporal recording of iceberg collective dynamics along the coast of Greenland; Section 2.4 presents the challenge of observing and modeling river bed dynamics from flood to flood. In these natural granular systems, as in experiments presented in Section 2.1, the stress – or energy – landscape in the system appears significantly changed after a failure event, leading to hysteretic behavior. Finally, Section 2.5 presents some of the major challenges in modeling the intermittency and near-criticality of volcanic processes from the fundamental scale of mineral crystals and gas bubbles.

2.1 Rigidity, nonlocality, and acoustics in dense granular materials – K. Daniels

Context. Forecasting the deformation and evolution of Earth's critical zone – whether through creep,[152] flow,[153] or catastrophic failure[154] – underlies many of the problems presented in this paper. Within the soft matter physics community, these questions have been addressed as questions of rigidity: how resistance to flow arises from the particle-scale to the meso-scale and to the system scale. Within a granular or amorphous material, internal stresses are transmitted by a heterogeneous network of forces known as force chains, as shown in Fig. 7. This network provides the material with its global rigidity, and several techniques exist for probing the spatio-temporal evolution of rigidity at various scales. Physicists have constructed models based on nearly-perfect particles residing within an energy landscape of valid states,[155] as well as simplified models comparing the number of constraints to the number of degrees of freedom.[156]
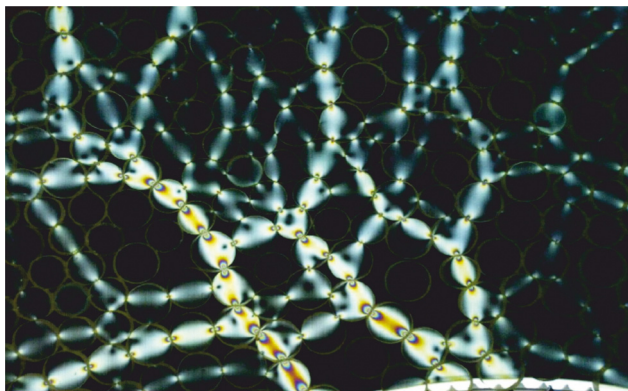
Fig. 7 An image of photoelastic disks (of $\simeq 1$ cm diameter) resisting a shear force applied by the roughened boundary visible at the lower right, imaged with a darkfield polariscope.[29,30] These methods allow for the quantitative determination of the vector contact forces between particles when performed in monochromatic light. In this image, the brighter particles are those carrying more force, while the darker particles carry little force. Under increased shear, the chains of forces buckle and rearrange (Source: E. Berthier, F. Fazelpour, C. Kirberger, NC State Physics).

Recent advances. For simplified laboratory systems, in spite of their dissipative nature and the difficulty of defining a frictional failure criterion, it now appears that the energy- and constraint-based frameworks both predict the same regions as being rigid or not.[157] When passively listening to acoustic emissions transmitted through the material, the statistical distribution of the resulting vibrational modes subtly shifts as a laboratory granular material approaches its point of failure,[158] as would be predicted for model materials developing low-frequency vibrational modes as they approach a state with zero rigidity.[159] Finally, for models of disordered solids – networks manufactured to have a disordered network of thin beams – it is possible to forecast the most likely failure locations using only the meso-scale topology of the network's connectivity, without including any mechanical information.[160]

Open questions. It remains an open question whether these frameworks can translate to the rough, heterogeneous, anisotropic particles and wet environments necessary to understand geophysical dynamics. For instance, is it possible to measure a quantity like the density of vibrational modes[161] using seismometers or strain sensors? When a hillslope or glacier progresses towards a critical point of failure, do similar hallmarks forecast likely failure locations and times? Already, network science has been successfully used to evaluate kinematic data obtained from ground-based radar, interpreted in light of the underlying micro-mechanics of granular failure, to successfully forecast the location and time of granular failure.[162]

2.2 Soft matter of post-wildfire debris flows – D. Jerolmack and N. Deshpande

Context. Visible and striking examples of near-critical behavior are the formation of post-wildfire debris flows and rockfalls. Both are increasingly frequent and deadly hazards that arise when hillslope soil and rock lose stability in the wake of intense burns. Debris flows are highly concentrated slurries of soil and water that form on steep hillslopes,[153,163] while ravel and rockfall are dry processes which occur when obstacles (*e.g.* vegetation) are removed or fail.[164] Predicting the conditions that will trigger this loss of stability, and assessing the hazard associated with their run-out, still rely largely on empirical relations derived from observations of previous flows. The challenges for understanding the mechanical stability of hillslopes in general and the failure and dynamics of debris flows also represent frontier challenges in soft matter science, and find a particular relevance in the context of post-wildfire conditions.

Recent advances. Historically, geoscientists have understood the failure and yield of Earth materials primarily *via* the Mohr-Coulomb criterion.[35] However, sub-yield creep is pervasive in soils[165–168] well below slopes where the Mohr-Coulomb framework would suggest motion. Surprisingly, it has been shown that even an undisturbed sandpile beneath the angle of repose creeps: this relaxation is very similar to aging in soft materials and glasses following application of a stress,[152,169] adding to growing knowledge and understanding of gravity-driven creep of (athermal) granular materials.[170–172] Probabilistic approaches grounded in statistical mechanics have in particular achieved success and insight, with the recognition that rockfall and ravel are dilute processes whose dynamics are akin to granular gases.[173–176] Once considered an outright myth because of complex fluid-sediment feedbacks,[177] a unified rheology for debris flows has been recently proposed,[153] where the key ingredients are a particular soil's packing fraction and distance from the jamming point.

Open questions. As applied to post-wildfire debris flows, a host of questions arise that require new soft matter physics knowledge to address. Some wildfires are known to leave behind a hydrophobic layer beneath the surface, which may help to confine rainfall to a shallow surface layer of soil that accelerates saturation and failure.[178–180] Rapid wetting of surface soils may also create strong capillary pressure gradients that regulate soil failure and erosion style. How do these processes affect soil creep? Do interfacial soil properties tune a hill's proximity to the jamming point? Debris flows may form by an unjamming transition in which soil experiences a sudden loss of rigidity associated with a decrease in volume fraction; *i.e.*, a landslide.[181] However, they also may form by progressive soil entrainment that increases volume fraction until it approaches the jamming point.[180,182] The conditions that lead to one or the other mechanism are not known. The rheology of debris flows is certainly non-Newtonian; generally, debris flows appear to be yield–stress materials with some degree of shear thinning.[183,184] However, rheology appears to be extraordinarily sensitive to the concentrations of clay and sand.[185] Concepts of jamming and lubrication are just beginning to be applied to heterogeneous debris-flow materials and offer some hope to explain and even collapse the variability observed in disparate studies.[153] Debris flows entrain large boulders that migrate to the front of the flow and act as a battering ram.[186,187] Whether this is the result of granular segregation like the Brazil nut

effect or a consequence of phase separation of granular (boulder) and liquid (mud) materials is unknown.

2.3 Floating granular materials – J. Burton and K. Nissanka

Context. Interfaces play a key role in many soft matter systems. Dense collections of surfactants, particles, and other contaminants confined to a liquid interface can have their own rheology and serve as a rigid boundary for flow near the surface. Although the Earth's oceans, seas, and rivers cover immense length scales, granular collections of ice, trees, organisms, and pollutants can play a similar role. These floating granular materials often jam in converging flows or narrowing geometries, creating hazards or ephemeral perturbations to the dynamics of Earth's aquatic interfaces. Examples include logjams,[188] river ice,[189] sea ice,[190] and volcanic pumice.[191] In biological systems, granular rafts can be formed intentionally to survive flooding, as in the case of fire ants.[192] Although the fractional coverage of Earth's water bodies with floating granular materials is small, they can be exceedingly important, since these crucial veins of transport can become quickly jammed with buoyant terrestrial debris.

Recent advances. Here, an outsized example of this behavior is showcased: ice mélange, a buoyant agglomeration of icebergs and sea ice that forms in the narrow fjords of Greenland (Fig. 8a). Ice mélange is perhaps the Earth's largest granular material,[193–195] with individual clasts ranging from 10 s to 100 s of meters in size. As ice mélange is slowly pushed through fjords that are many kilometers wide, it jams, buckles, and breaks as friction from the rocky walls transmits stress to the buoyant interior. Most of the time, ice mélange flow is quiescent, and quasistatic. As a granular material, it is near-critical and the inertial number is much less than unity.[196] Similarly, from a rheological perspective, the material creeps along near the yield criterion for flow. This means that large fluctuations in forces, that can't be captured by most continuum models, can develop. Importantly, this quiescent flow can be punctuated by large discharges of icebergs into the glacial fjord, known as iceberg calving. During calving, cubic-kilometer-sized icebergs are fractured from the main glacier and often capsize into the ice mélange.[197,198] Moreover, ice mélange has recently been shown to affect ice-sheet mass losses by inhibiting iceberg calving.[199] Surprisingly, centimeter-scale iceberg displacements can be measured with ground-based radar every 3 minutes. These measurements reveal that a period of incoherent granular flow precedes iceberg calving events (Fig. 8b), representing an important first step towards real-time detection of failure in geophysical granular systems.

Open questions. Within the context of floating granular materials, there remain a few key challenges. These materials are very sensitive to particle shape and confinement, both of which are essential for their ability to jam and transmit stress. Examples like ice mélange are confined by rigid fjord walls, but are unconfined and stress-free near the open ocean. Also, these materials can interact with the water, e.g., melting ice drives stratified flows from below, but can also cool the surface waters and enhance the formation of sea ice in the winter. Finally,
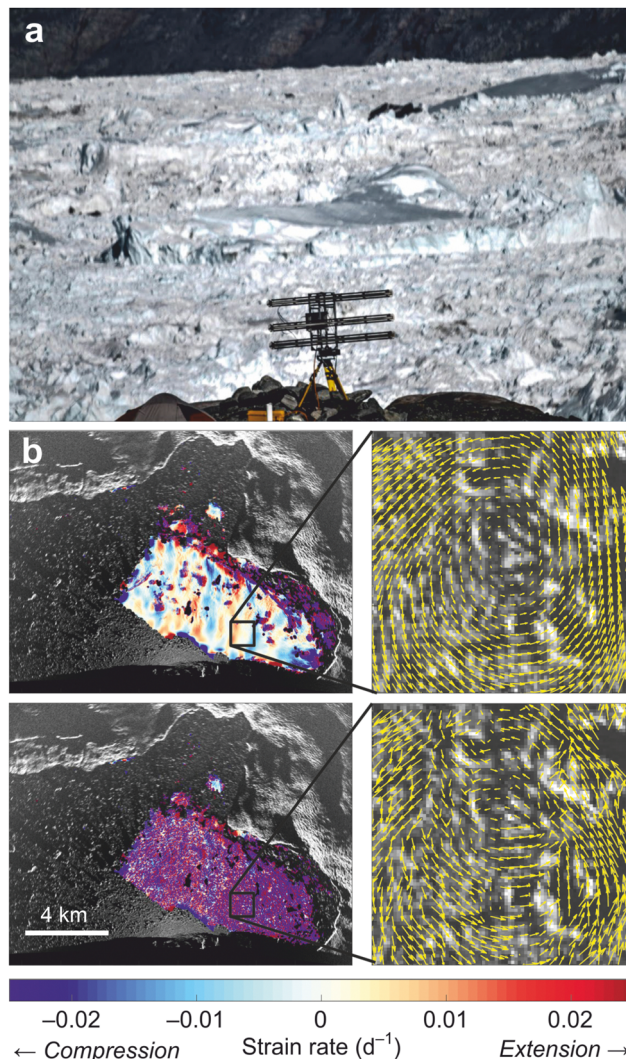

Fig. 8 Adapted from Cassotto et al.[199] (a) View of ice mélange at Sermeq Kujalleq (Jakobshavn Isbræ) on the Western coast of Greenland. The ground-based radar visible in the center of the image is a few meters in size and is perched on the rocky cliffs above the fjord. (b) Top-left, divergence of velocity field under steady flow. Red areas represent extension of the flow, and blue areas represent compression. Overall, the field is smoothly varying. Top-right: Variation of velocity field in the black rectangle after subtracting the mean of the underlying steady flow. Bottom-left, divergence of velocity field less than 1 hour before a calving event (the fracture and discharge of a cubic-kilometer-sized iceberg from the glacier into the ice mélange). The divergence field is rapidly-varying and noisy. Bottom-right: variation of velocity field before calving, showing heterogeneous flow patterns.

laboratory studies combined with continuum modeling using nonlocal granular rheologies are needed to provide a larger-scale picture of how floating granular materials shape and respond to their dynamic environment.

2.4 River sediment beds remember past flows – C. Masteller

Context. Erosion and morphological change in gravel-bed rivers arise through bedload transport: rolling, sliding, or saltating close to the riverbed. Almost all existing model

predictions of bedload transport rates are underpinned by the degree to which flow conditions exceed some critical value in dimensionless shear stress,[200–203] representing either the initiation of motion of sediment particles,[204,205] or some "reference" transport rate.[206,207] For gravel-bed rivers, the bulk of sediment transport occurs close to these thresholds.[206,208,209] In the context of soft matter, fluvial transport processes near the stream bottom can be viewed as the dynamical evolution of a granular system near criticality.

Recent advances. It is known that there is a strong link between the width of a river when filled to the top of its banks (bankfull), and the entrainment threshold of bed and bank sediments above which transport begins. Near-threshold channel theory (NTC)[206] is a model for this process which has been validated for several different types of rivers.[208–211] While most bedload transport models use a constant dimensionless shear stress, σ_c^* (or critical Shields stress), as the threshold parameter, it is now understood[212] that such a universal threshold should be applied with caution. For example, field measurements show that longer inter-flood duration may lead to increases in σ_c^* and reduced sediment transport rates.[213]

Laboratory experiments confirm that the magnitude and duration of inter-event flows affect σ_c^* evolution and show that with little to no active sediment transport, grain-scale changes in interlocking, and subtle surface reorganization increase particle resistance to motion.[214,215] These observations suggest that the increase in particle resistance under inter-event flows is akin to granular creep and compaction of granular materials under low to moderate shear rates. In response to higher magnitude flows (*e.g.*, floods) surface reorganization of the bed leads to a decrease in particle entrainment thresholds *via* an increase in surface roughness, akin to dilation of granular materials under high shear rates.

A high-resolution, multi-year time series of entrainment critical stress, σ_c^*, from the Erlenbach torrent, a mountain stream in Switzerland,[216] revealed that the magnitude of antecedent flows was the dominant control on the evolution of σ_c^*, with a secondary, short-lived duration effect.[217] Consistent with laboratory experiments,[218,219] these direct measurements showed increases in σ_c^* with increasing inter-event flow magnitude. In higher-magnitude, sediment-transporting flows, strengthening effects were also observed following low to intermediate-magnitude bedload-transporting floods; however, following high-magnitude flows, σ_c^* for motion decreased.[217]

Open questions. A flow history-dependent empirical model in which σ_c^* evolves through time as a function of bed shear stress can be used to capture these variations in particle erosion thresholds.[220] A more fundamental, particle-scale-based approach could provide more insight. One possible explanation for the observed history-dependence[217] is that the transition from bed strengthening to bed weakening is associated with a transition from sparse local rearrangement of particles to a more established sediment transport flow, capable of significantly disrupting bed structure *via* particle collisions or long-distance particle transport.[221]

Another key challenge requiring a soft matter approach is to better understand how deformable boundaries (such as river bed channels) respond to variations in bed shear stress σ^*, and by extension, to variations in σ_c^*. Dilation occurs at shear stresses well above those commonly observed to result in channel widening,[171] suggesting that bed disruption or weakening may be infrequent or buffered by channel width adjustments. Thus, further exploration of the feedbacks between adjustments in σ_c^* and channel widening onset should be explored.

Further afield, definitive links between granular processes observed in laboratory experiments and field observations in gravel-bed rivers are precluded by various technical limits. The difficulty to acquire accurate *in situ* measurements of complex shapes of natural grains, fine-scale dynamical changes of grain-scale topography,[222] grain motion beyond the bed surfaces, and small changes in σ_c^* values are some of them. Indirect geophysical methods, including environmental seismology[223–226] and distributed acoustic systems,[227] which are currently explored in fluvial contexts, could allow bypassing some of these limits and connecting the dynamics over the different scales of the river-channel granular system.

2.5 Why do persistently degassing volcanoes erupt? – J. Suckale

Context. Volcanic eruptions are perhaps one of the most dangerous examples of multiphase soft matter dynamics. Eruptions are driven by gas bubbles dissolved in magma, or the interaction of magma with water and steam. During eruptions, the surrounding porous rock can fragment and form a fast-flowing granular material, and magma often contains crystal-rich and crystal-poor regions, making it a heterogeneous and complex fluid. Most volcanoes display intermittent dynamics, a common feature of many soft materials driven by external stress; yet not all volcanic eruptions are rare. According to the Volcano Watch by the United States Geological Survey, dozens of volcanoes erupt every day, sometimes repeatedly. These volcanoes are commonly referred to as persistently active: due to an open connection between the magma storage regions and the surface vent a dynamic system arises. Their volcanic activity spans a wide spectrum from continuous passive degassing to intermittent explosive or effusive eruptions with more violent, paroxysmal eruptions emerging with little or no clear precursory activity.[228,229] The transitions between different eruptive regimes are sudden and unpredictable, creating large uncertainty in risk assessments.[230] In fact, the National Academies declared the development of multi-scale models that capture critical processes and can be tested against field data as one of the three grand challenges in modern volcanology.[231]

Recent advances. Near-criticality lies at the heart of understanding the eruptive regime transitions. Most of the time, persistently active volcanoes are not erupting and still emitting copious quantities of gas and thermal energy;[232–237] why not always? Near-critical behavior of the magma can provide a valuable framework for understanding why seemingly small increases in gas flux, pressure or crystallinity could lead to a sudden and dramatic change in behavior. For example, direct

examination of ejected materials reveals that the uppermost few hundred meters of the plumbing system at Stromboli volcano, Italy, are composed of a highly crystalline mush with a solid fraction of 45–60%.[238–240] This 'magmatic' mush is prone to tensile failure beneath the observed vent locations driven by gas overpressure and the tectonic stress field, suggesting that Strombolian eruptions could be related to a transition from flow to failure.[241] Yet, a transition from distributed flow to localized failure can also occur in flow configurations with low crystallinity. One process that could trigger such a transition even in a largely fluid system is the hydrodynamic interaction between individual crystals.[242] The hydrodynamic interactions between crystals are amplified by the high viscosity of magmatic melts, roughly five to twelve orders of magnitude higher than water, because it implies that individual crystals interact hydrodynamically over spatial distances many orders of magnitude larger than their size. These long-scale hydrodynamic interactions between individual crystals favor the development of correlations in the spatial distribution of crystals which both depend on the ambient fluid flow field and also modify it.[242–244]

Fig. 9 shows an example of a lava fountain during the 1959 eruption at Klauea Iki, Hawaii, and a close-up photo of the crystal clusters later found in erupted samples.[245] This crystal cluster formed by two particles drifting together during flow and intergrowing over time.[245] The puzzling aspect of such crystal clusters is the abundance of relatively large misalignment angles separating the two crystals.[246] A smaller angle would be hydrodynamically more favorable, but is only observed in a surprisingly small percentage of clusters. However, it is known that in linear shear flows, particles tumble along in Jeffery orbits,[247] but wavy flows align crystals[248,249] towards a preferential angle that depends on both the flow conditions and the particle geometry. As such, observations of crystal geometry suggest that the high percentage of large misalignment angles is indicative of a downward propagating wave in a volcanic conduit with low crystallinity.[250] The inferred crystallinity is consistent with the lower range of observed crystallinities[251] and with the possibility that a spatially heterogeneous arrangement of crystals inside the volcanic conduit could trigger a transition from flow to localized sliding over a thin interfacial layer within the magma mixture.[242]

Fig. 9 Photo of a lava fountain during the 1959 Kilauea Iki eruption (courtesy of USGS) in the background and a photo of a crystal cluster later identified in erupted samples by Schwindinger and Anderson.[245]

Open questions. Testing different models directly against data will provide knowledge of the variety of physical processes that can disrupt conduit flow, reflected in the diversity of observed eruptive regimes. Some of the most precious clues may emerge at the micrometer scale, from observing crystals or bubbles, because this data may directly record at least some pre-eruptive processes.[250] Lending a helping hand in preserving this information is the glass transition, a unifying theme in soft and disordered materials. Once the eruption starts, the melt in the conduit quenches to a glass, freezing-in the crystals and bubbles it contains.

Many questions and challenges regarding the eruptive behavior of persistently active volcanoes remain, and require expertise outside of classical volcanology: multi-phase flow, nonlinear dynamics, thermodynamics, and numerical analysis. These challenges touch on several themes discussed in this paper, particularly the challenge of modeling the grain scale (1) and the challenge of bridging scales (3). Like many other natural systems, volcanic systems span an enormous range of physical conditions and scales from microns to hundreds of kilometers.

3 The challenge of bridging scales

Earth surface processes occur over a vast range of scales, from the near instantaneous transport of millimeter-sized sand grains in a stream to the slow drift of entire continents over millions of years. Further, Earth materials that are seemingly solid on short timescales (*e.g.*, soil, rock) can behave like soft materials over long timescales (*e.g.*, soil creep, convection of Earth's mantle). This results in unique challenges in our ability to directly observe Earth surface dynamics in the field, highlighting the need for ways to use experiments and models at shorter length and time scales to better understand dynamics at larger, geologically relevant scales (Fig. 1). This section highlights some recent studies that use a combination of experiments, remote sensing, fieldwork, numerical modeling and theory to understand how small-scale dynamics lead to large-scale patterns and behavior, leveraging connections between Earth and soft matter systems.

Section 3.1 highlights that mechanisms of viscous and elastic deformations might differ in the temporal and spatial domains, in the specific case of Antarctic ice dynamics. Section 3.2 tests if rainfall time signals, modulated in space *via* groundwater flow, can be approximated by averaging over time. Such results highlight the importance of fluctuations in Earth science, which do not simply add noise but act as a fundamental feature on Earth's surface and in other nonlinear systems. Section 3.3 considers the complex fluid dynamics at the bottom of glaciers as it relates to reactive porous media flow, exploring how to reproduce the evolution of subglacial channel systems, coupling models of sediment transport and ice melting. Section 3.4 focuses on understanding how porous media convection and physicochemical mechanisms in the ground result in the striking formation of surficial salt patterns.

Section 3.5 presents a scaling analysis and remote sensing measurements of Arctic soil patterns and investigates their similarity to fluid–flow instabilities. Finally, the dynamics of dunes – fragile but perpetual forms in deserts – remains challenging to predict; Section 3.6 uses laboratory-scale experiments to show how dunes persist and set a length scale in landscapes by interacting, attracting, and repelling each other.

3.1 Ice cracks in a warming climate – Y. Lai

Context. Interactions between fluids,[252–260] elasticity[261–265] sediments,[266–268] granular flows,[193] and porous flows[269–271] are ubiquitous in polar regions. Ice sheets and ice shelves are viscous gravity currents spreading over bedrock and oceans,[254] respectively. Ice is a complex material that exhibits scale-dependent characteristics of soft matter, flowing as a viscous fluid (*e.g.*, glaciers) at longer timescales, but breaking as a solid at shorter timescales (*e.g.*, iceberg calving[272,273]). Because the mass loss of ice contributes to the rising sea-levels, it is important to understand the fate of ice sheets and shelves in a changing climate. Here, a few processes involving interactions between fluids and solids with important implications for ice dynamics are highlighted.

Recent advances. Atmospheric warming threatens to accelerate the retreat of the Antarctic ice sheet by increasing surface melting and facilitating hydrofracturing,[274] where meltwater flows into and enlarges fractures on ice shelves,[275,276] potentially triggering ice shelf collapse[274,277,278] and acceleration of sea-level rise.[279] Fig. 10a illustrates a theoretical prediction of the stability of Antarctic fractures depending on the ice thickness, ice toughness, and glaciological stresses on ice shelves. To compare observations with theory, a deep convolutional neural network was utilized to detect continent-wide fracture features on ice shelves.[8] Most ice shelf locations that the deep neural network detects as fractures, shown as points in Fig. 10a, lie in the parameter regime where our theory predicts stable

fractures (gray triangle), and are consistent with the fracture theory. Due to the ubiquity of fractures on ice shelves, if climate warms and causes the Antarctic ice surface to melt, large portions of Antarctic ice shelves will likely collapse due to hydrofracture.[8]

Besides theory and field observations, analogue experiments can make a unique contribution to the understanding of ice sheet processes. The benefit of analogue experiments is that essential parameters can be well controlled. The findings in analogue experiments can be connected with the large-scale geophysical observations by matching the relevant nondimensional parameters. For example, laboratory analogue experiments have been developed[280,281] to mimic the formation and relaxation of a water-filled "blister" (Fig. 10b) beneath an ice sheet due to the injection of meltwater.[282] The analogue experiment[280,281] (Fig. 10c) validated a mathematical model describing meltwater leaking from a pressurized "blister" into the surrounding water network (modeled as a porous substrate) beneath the ice sheet (modeled as an elastic sheet). The mathematical model has been used to constrain the hydrological property of the water network beneath the ice sheets, which is otherwise difficult to measure.[280]

Open questions. Many unanswered questions are to be explored, such as the processes governing the catastrophic collapse of ice shelves, including the mechanisms responsible for the periodic undulations observed in satellite imagery (Fig. 10d). The surface periodic undulations are highly correlated with locations of basal crevasses or large fractures.[283–285] While the undulation spacing is relevant to the size of icebergs, the types of mechanical instabilities[286] that give rise to these periodic patterns are still poorly understood (Fig. 10e). The effects of complex rheologies of Earth materials (ice, sediment) on the mechanical instabilities, the disintegration of ice shelves, and the dynamics of ice sheets, remain scarcely investigated.
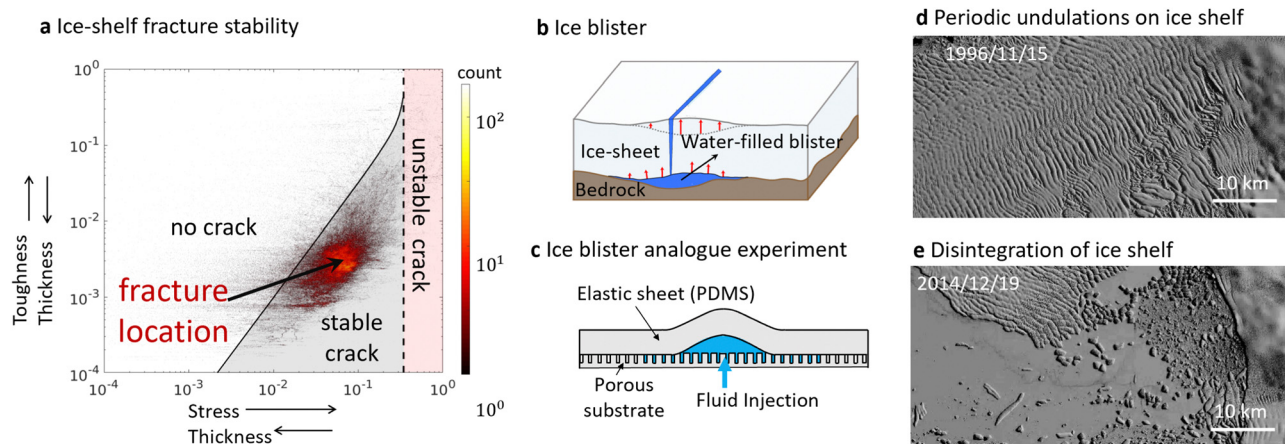

Fig. 10 (a) Fracture stability diagram for Antarctic ice shelf fractures. Most ice shelf fractures identified by a neural network on Antarctic satellite imagery (red dots) lie in the stable-fracture regime. Adapted from Lai *et al.*[8] (b) Formation of water-filled "blister" at the bottom of the ice sheet after a lake drains. Adapted from Lai *et al.*[280] (c) Analogue laboratory experiment mimicking a water-filled blister beneath an ice sheet relaxing on a porous water network.[281] (d) Satellite image showing undulation patterns on ice shelves due to fracture formations on the Thwaites Ice Shelf in 1996. (e) Same region as (d), in 2014 when the ice shelf was broken into icebergs ((d) and (e) are from Landsat image).

3.2 Can the groundwater flow be time averaged? – O. Devauchelle

Context. A central challenge in bridging small to large temporal scales in non-linear systems, like the ground beneath our feet, lies in finding a meaningful average from inherently noisy or fluctuating data. A key example in Earth science is the statistical analysis of stochastic rainfall rates and subsequent groundwater flow. Rainwater infiltrates into the ground, until it reaches the water table, where the porous matrix is saturated with groundwater (Fig. 11). There, it begins the slow underground travel that will eventually bring it back to the surface, where it will join a stream, and run to the sea. How long does the subsurface part of this travel take? The residence time of water in an aquifer is $\tau = \dfrac{V}{RA}$, where V is the groundwater volume, A is the area of the catchment, and R is the rainfall rate[287] (typically expressed in mm year^{-1}). Residence time is thus tantamount to storage. It is also a prime control on the biological and chemical reactions that weather the porous matrix, and a good estimate of the time it takes for groundwater to recover from pollution.[288,289] It is therefore crucial to the management of water resources, and to the understanding of the vadose zone and therefore of the global carbon cycle.[290,291]

Recent advances. As a first approximation, one can average rainfall over years, and treat its mean $\langle R \rangle$ as a steady forcing of the groundwater flow. The resulting Darcy problem is then stationary and amenable to classic fluid mechanics. For illustration, Fig. 11 shows the stationary flow of groundwater through deep, unconfined aquifers that discharges into neighboring streams.[287] As the rainfall rate increases, the water table rises. The domain over which the flow equations need to be solved thus expands, and this makes the problem non-linear. Even in steady-state, the residence time of water in an aquifer is not just inversely proportional to the rainfall rate, because the volume of groundwater needs to accommodate the flux it carries – V is a function of R, and the determination of this function is still an open problem.[287,293]
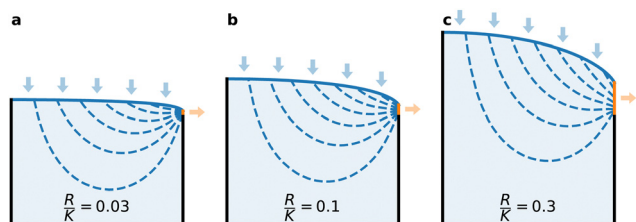
Fig. 11 Analytical solutions of flow in unconfined aquifers, of different volumes and water table heights (increasing from (a)–(c)) of hydraulic conductivity K recharged by a constant rainfall R.[292] Rainwater infiltrates into the ground (blue arrows), and joins the water table (solid blue line). From there, it follows the groundwater flow lines (dashed blue lines) until it reaches the outlet (orange line), where it seeps into a river. The river flows towards the reader. The solid black lines are impervious (left: groundwater divide, right: axis of symmetry). All lengths are made dimensionless with the distance that separates the river from the divide. There remains only one dimensionless parameter in this problem: R/K.

In reality, of course, precipitation is intermittent, and so is the rainfall it generates. Since the groundwater flow is non-linear, one cannot expect that a time average will gracefully propagate through the equations, as it would in a linear system.[294] Therefore, there is no reason to believe that the steady flow of Fig. 11 is the average of the actual groundwater flow. To find the latter, one generally needs to solve the non-stationary problem, and average the result over time – a procedure far more costly than solving the steady-state problem. In short, finding the average groundwater flow is a difficult problem, because it is not just the solution of the average equations. There is a simple solution to this problem when the groundwater flow is very shallow: the steady-state solution gives the root mean square of the storage volume.[294] This solution, unfortunately, breaks down when the groundwater flow extends deep into the ground.

Open questions. This problem, which might seem anecdotal, is in fact ubiquitous. One simply needs to consider a non-linear system driven by some fluctuating forcing. For example, sediment transport in rivers depends on turbulent fluctuations in the fluid flow and stochastic interactions between grains.[295] In cold climates, soil cycles through freezing and thawing due to temperature fluctuations (Section 3.5), modulating its rheology, and therefore its downward creep (Section 2.2).[172] Could this parametric forcing explain why some soil patterns appear only in the Arctic? (Section 3.5). Recent work has begun to formally examine Earth surface processes in a probabilistic way, treating stochasticity not simply as noise, but as a fundamental feature of these systems.[176] In other words, fluctuations do not always average out. In Earth sciences, this might be the rule rather than the exception.

3.3 Subglacial drainage as a reactive multiphase flow – I. Hewitt

Context. Fluid-sediment interactions beneath thick ice sheets and glaciers are key to our understanding of glacier dynamics. Yet, like many Earth surface phenomena, their dynamics span large spatial and temporal scales and are very challenging to observe directly. Increased glacier and ice-sheet melting is an obvious consequence of climate warming, with significant impacts for sea-level rise and for water resources in mountainous regions. Vast quantities of meltwater are transported beneath the ice, along the interface between ice and the underlying bedrock or till (sediment deposited by the ice), driven out towards the ocean by the overlying weight of the ice. With little opportunity for direct observations, various conceptual theories for how to envisage the subglacial drainage system have been developed. There are similarities, and some important differences, to surface water flow and stream formation, as well as links to reactive porous media flow, in which the porous medium (in this case ice) can deform and change its internal structure through time.

Recent advances. An important aspect of these systems is their temporal evolution – it is inferred from tracing experiments that there is a massive expansion of the drainage system during the summer melt season (due to dissipation-driven

melting of the basal ice), but that this subsequently collapses (due to the viscous "creep" flow of the ice) during the winter.[296] The system is believed to transition between a relatively low permeability system in which water moves through porous sediments or "linked cavities", and a more efficient river-like network of channels.[297] The channels can be incised both upwards into the ice[298] and downwards into the sediments.[299]

One aspect of these channels is that they are believed to be responsible for depositing eskers (Fig. 12). Eskers are long, sinuous ridges of sand and gravel, found particularly in areas of Canada and Scandinavia, which were deposited as the ice sheets retreated at the end of the last glacial period. Suggested formation mechanisms for an esker include continual deposition at the widening mouth of the channel as the ice sheet margin retreats.[300] Sediments are deposited as the flow velocity in a water-filled subglacial channel decreases near the retreating ice margin. The spatial distribution of the sediment size dependence on the flow velocity might be used to test this hypothesis. A better understanding of the formation mechanism of eskers can inform more about the plumbing system under present-day ice sheets.

Open questions. Open questions abound about the relevant physics, and how it can be modeled. In particular, these include the role of erosion, deposition, ice-melting, and ice creep in enlarging and contracting the space available for water to flow under and through the ice. There are potentially useful analogies with other deformable or reactive porous media, and for an increased role for analogue laboratory experiments.

3.4 Patterns in dry salt lakes – L. Goehring

Context. Dry salt lakes, playas, and salt pans represent some of the most extreme environments on Earth. They form in dry terminal basins where groundwater collects just beneath the surface of the soil and where evaporation dominates over precipitation.[301] The otherworldly landscapes that result are ones of beautifully ordered polygonal patterns that decorate a surface salt crust, and are an inspiration to fantastic settings like Star Wars' planet Crait. Found worldwide, some noteworthy dry salt lakes include Badwater Basin in Death Valley
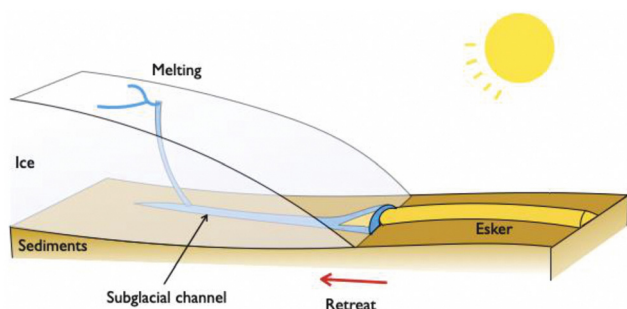
Fig. 12 Suggested formation mechanism for an esker. Eskers are long ridges of sediment, which were deposited as the ice-sheets retreated at the end of the last glacial period. Sediments are deposited as the flow velocity in a water-filled subglacial channel decreases near the retreating ice margin.

(CA, USA, Fig. 13a), Salar de Uyuni (Bolivia), Dasht-e Kavir (Iran), and Sua Pan (Botswana). The example of Qaidam Basin, China, has also been studied as an analogue for strikingly similar features found on Mars.[302] Although fracture[303] and buckling[304] of the surface crust are associated with these features, until recently, no clear mechanism has been able to accurately explain the emergent spatial and temporal scales of the salt crust patterns. The main challenge to any such explanation involves identifying a mechanism specific to salt lake environments that can account for the consistent growth of 1–3 m wide closed polygonal features in the crust,[305,306] over timescales of a few months,[305,307] and in a way that is insensitive to the exact salt chemistry and soil composition of any particular lake site.

Recent advances. In order to predict the formation and dynamics of salt crust patterns, an intimate link between these dynamics and the convection of salty water within the soil has been proposed, where convection cells template the crust pattern.[308,309] Convection in porous media is itself well-studied, with a variety of approaches and applications summarized in a recent, extensive review.[310] In the context of salt crusts, the connection is made to the particular problem of convection in the presence of a through-flow of fluid. This problem was originally raised in the context of geysers,[311] but has since been developed to explain the subsurface flows observed at playas or dry salt lakes[312] and sabkhas, which are evaporate pans near tidal flats.[313]

Briefly, the resulting model considers the Darcy flow of water in the porous sand or sediment of a dry lake, where the water table remains close to the surface of the ground.[308,309] The water contains salt, which accumulates at the evaporating surface. The salt moves advectively with the water, and diffusively along any concentration gradients. It adds to the density of the water, providing buoyancy forces that can drive additional flows. As boundary conditions, there is a continuous loss of water at the surface, caused by evaporation, and the groundwater is recharged from below by some distant reservoir. This leads to the accumulation of salt-rich, denser water near the surface, which can be unstable to convection. The convective dynamics are captured by a single dimensionless group, the Rayleigh number, which describes the ratio of convective to diffusive effects. Essentially, this group describes the vigor of any convection,[308] as it also characterizes the speed of the convective flows, relative to the background flows caused by the surface evaporation.

Building on a body of recent field observations,[305,306,309] this model of a salt playa allows for the dynamic evolution of convection cells, which then modulate the salt flux into the surface crust.[309] As confirmed by direct field data of crust growth rates[305] and subsurface flow patterns,[309] it predicts that surface salts will accumulate fastest above down-welling flows that spontaneously arrange into a polygonal network (Fig. 13b and c) when simulated in large, three-dimensional domains.[309] When the model parameters are constrained by relevant field data, it also accurately accounts for the observed growth rates of the polygons, and their remarkably consistent size, which
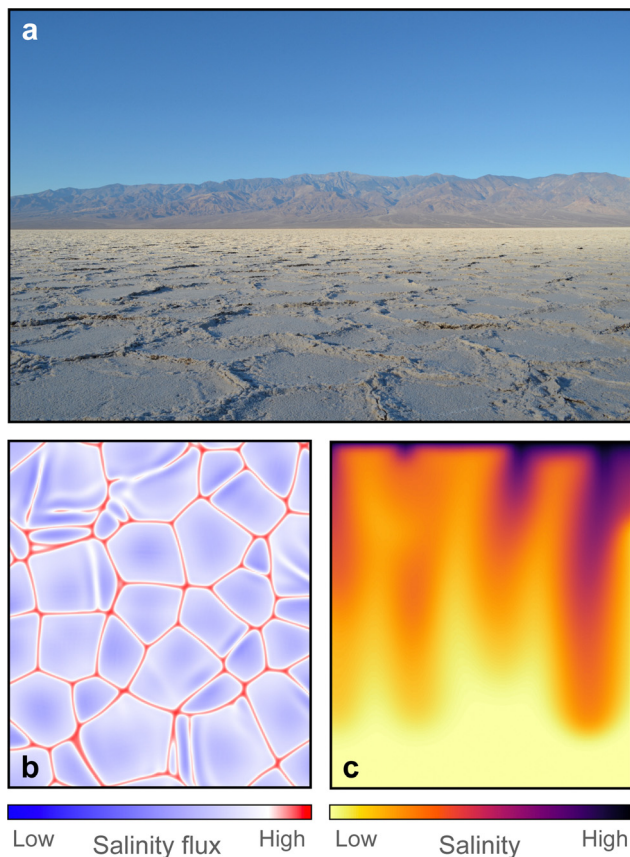
Fig. 13 A convective model of salt polygons in dry salt lakes. (a) The dry lake surface at Badwater Basin, Death Valley (CA, USA), is covered by a pattern of ridges in an approximately 10 cm thick crust lying over moist sandy soil. Here, the polygonal features are typically about 1.5 meters across. The model of buoyancy-driven flows used to simulate the emergent length scales and time scales of pattern formation at such sites predicts (b) salt flux into the salt lake's crust (and hence crust growth rates), and (c) salinity vertical profiles underneath. Panels (b) and (c) courtesy of and copyright Matthew Threadgold.

arises naturally from a balance between evaporation rates and salt diffusivity.

Open questions. Further development of these ideas would require considering more carefully the feedback between the crust and the groundwater flows and accounting for how the development of differences in crust thickness will, in turn, influence local evaporation rates.[308,314,315] This effort would not only contribute to the understanding of these patterns but also to environmental impact. For example, Owens Lake has been the focus of a decades-long remediation effort to reduce dust formation off of dry lake surfaces, which is linked to the dynamics of the salt crusts.[314] However, even without further elaboration, the convective model demonstrates how the self-organization of flows beneath our feet can naturally explain the emergent length scales and time scales of salt polygons in nature.

3.5 Fluid-like patterns in slow-moving soils – R. Glade

Context. A key challenge in linking soft matter physics with Earth science lies in dealing with the high degree of heterogeneity in natural landscapes.[176,316] In cold landscapes, icy soil composed of an ever-changing mixture of heterogeneous sediment grains, liquid water, and ice demonstrates the complexity of Earth materials.[5] Soil in these settings moves downhill at slow rates of millimeters to centimeters per year due to freeze–thaw processes (e.g., ref. 317); over time, the soil self-organizes into distinct finger-like patterns known as solifluction lobes, with wavelengths of tens to hundreds of meters (Fig. 14). Despite their ubiquity in cold regions, the necessary and sufficient ingredients to form these slow-moving soil patterns are unknown.

Recent advances. Inspired by contact line instabilities in thin film fluids (e.g., paint dripping down a wall) that form due to competition between viscous forces and surface tension (e.g., ref. 318), Glade et al.[319] develop a theoretical prediction for solifluction lobe wavelength that aims to connect grain-scale cohesion and fluid-like motion of the soil to large-scale pattern development while acknowledging the importance of natural heterogeneity. Similar to surface-tension dominated flows, competition between body forces and resisting forces (here in the form of enhanced soil cohesion at raised soil fronts) may drive pattern formation. Allowing for a hydrostatic component to account for large scale topographic roughness not present in thin films, a new scaling relation was found that predicts the cross-slope wavelength (λ_c) varies as a function of soil thickness (h), topographic slope ($\sin\theta$), and a length scale characterizing spatial variations in cohesion (ℓ_c): $\lambda_c \propto \sqrt{h\ell_c/\sin\theta}$.

Applied to remote sensing data of thousands of solifluction lobes across Norway, the theoretical scaling relation is able to predict average wavelengths.[319] Typical of field data, the solifluction wavelengths contain a large amount of scatter. Data show that average lobe heights and wavelengths also increase with elevation and decrease with mean annual temperature, pointing toward a broad climate control on solifluction patterns and illustrating the possible importance of external driving factors in addition to smaller-scale soil dynamics. This work demonstrates that even granular material in the non-inertial regime can exhibit instabilities fundamentally similar to those found in small scale systems, at time and length scales orders of magnitude larger than previously observed. The presence of these patterns only in cold landscapes suggests that the exceptionally large amount of heterogeneity found in icy landscapes may allow for the development of sub-critical instabilities in non-inertial flows.

Open questions. These findings point toward the need to address key knowledge gaps that impact our ability to understand landscape dynamics through a soft matter lens. First, there is a lack of adequate rheological models that can account for (i) the non-inertial regime,[320,321] (ii) heterogeneity in grain size and material properties,[322] (iii) cohesion between grains,[323] and (iv) the presence of liquid water and ice.[324] While a highly simplified treatment of soil creep as a viscous fluid works surprisingly well to explain average pattern wavelengths, without a more accurate representation of soil rheology, predictive capabilities are severely limited. Second, field observations of soil transport processes are difficult to obtain because
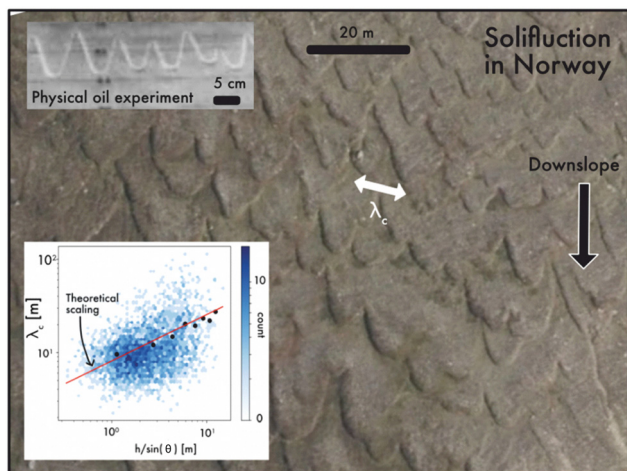
Fig. 14 Background: Aerial image of solifluction lobes with wavelength λ_c of tens of meters in Norway (image credit: The Norwegian Mapping Authority). Top left inset: Fluid contact line instability in a laboratory experiment with wavelength of centimeters.[318] Bottom left inset: λ_c plotted against lobe thickness divided by topographic slope, $h/\sin\theta$, measured from a remote-sensing derived digital elevation model. Blue color indicates the number of data points in each hexagonal bin. Black dots represent average wavelengths binned by $h\sin\theta$. Red line is theoretical prediction from fluid-inspired scaling analysis, $\lambda_c \propto \sqrt{h\ell_c/\sin\theta}$. Because there are no constraints on the cohesive length scale, ℓ_c, here it is assumed to be constant. Figure modified from Glade *et al.*[319]

they operate over long timescales, though recent advances show promise for obtaining high-resolution surface deformation of slow-moving solifluction lobes.[325] This illustrates the necessity for a collaborative, holistic approach that incorporates theory, laboratory experiments, numerical modeling, and field observations to better bridge grain-scale dynamics with landscape-scale processes and patterns.

3.6 Bedform dynamics: interaction, attraction and repulsion of dunes – N. M. Vriend and K. A. Bacik

Context. In desert landscapes, one can observe individual sand dunes of different sizes, with a characteristic length scale of up to kilometers, which seamlessly interact with each other and their environment.[326–328] As migrating sand dunes notoriously bury human-made infrastructure and lead to degradation of arable land, this interaction has important practical implications.[1,329] From a physical point of view, the evolution of a sedimentary surface is a result of an intricate coupling between the turbulent flow and the granular bed.[330,331] Relevant scales of motion in this system span several orders of magnitude, from sediment transport, through dune migration, to large-scale organization of a dune field.[332]

Recent advances. Here, the focus is on the system-level dynamics, which in the field occur over decades and thus are difficult to investigate in detail. However, in the lab, by using appropriately scaled miniature subaqueous dunes, these key physical processes can be investigated in a matter of hours. Specifically, three research questions are introduced here, which have been recently investigated within a new laboratory
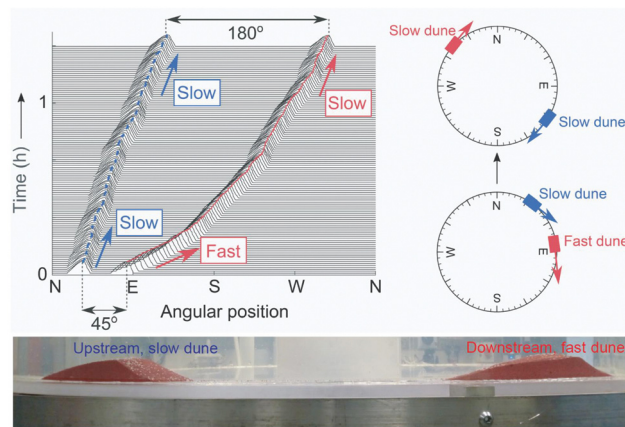
Fig. 15 Two equal-size miniature dunes are initially placed 45° apart in a periodic annular channel. Due to drag imposed by the water current, they start migrating and drift apart, and converge over long times to a symmetric antipodal configuration 180° apart.[333]

experiment (Fig. 15) uniquely suited for probing long-term dynamics due to its circular quasi-2D geometry.[333]

First, pairwise interaction between two dunes is explored, leading to either coalescence (merging), ejection (sediment exchange),[334] or wake-induced repulsion of bedforms[333] which can be categorized in a phase-space diagram outlining the possible interaction outcomes derived from experiments and cellular automaton simulations.[335] Second, as a first step towards understanding the system-level dynamics of a dune field, the long-term behavior of a periodic two-dune system[336] is investigated: is this system always attracted to a symmetric state with two identical equi-spaced dunes, or are there conditions where the symmetry is spontaneously broken? The key to understanding the dynamics is turbulence: for flows with a relatively low turbulence intensity, the dunes will display fast-slow dynamics before settling at a stable equilibrium, but for high levels of turbulence an asymmetric attractor appears. This indicates that, at least in theory, the hydrodynamic coupling between neighboring dunes can either promote or inhibit regular organization of a dune field. Third, by placing idealized objects in the path of the model dunes, the engineering challenge of dune-obstacle interaction are addressed. Interestingly, both object size and shape of the obstacle determine whether the dune is blocked or able to overcome an obstacle and reform on the other side,[337] and once again, the importance of turbulent flow structures is established. Indeed, the outcome of the dune-obstacle interaction can be predicted with a simple data-driven tool based on the modal decomposition of the flow field around the obstacle (without sediment or dunes present).

Open questions. Surprising connections between rapid small-scale processes (such as turbulent fluctuations interacting with a granular interface) and the slow large-scale evolution of sedimentary landscapes are revealed. Remarkably, by taking advantage of scaling laws, these processes have been investigated in a controlled laboratory experiment; validating these

predictions with observational data using remote sensing remains to be done.

4 The challenge(s) of life

Life has an impact on the dynamics and is impacted by the physicochemical evolution of the ground. Over time, plants, fungi, and burrowing animals alter the ground composition, constitutive structure, and consequently, its mechanical properties (*e.g.*, Fig. 1e). Sometimes the presence of life makes the ground more cohesive and enhances its resistance to erosion, sometimes its own dynamics pull apart or alter the ground such that it is destabilized. Such puzzling observations illustrate why it is crucial to isolate and study the biophysical processes happening in the ground. We present here two examples of such studies: in Section 4.1, recent results and outlooks on the dynamics and impact of invertebrates (such as worms) in the ground are presented, while Section 4.2 highlights a newly recognized effect bacteria can have on fluid dynamics in porous media. Finally, Section 4.3 presents recent results to support a fundamentally different usage of the ground as a resource; it reminds us that human beings, *via* the building of our infrastructure, are also a major part of the life disturbance of the Earth's ground and atmosphere.

4.1 Intruder dynamics in granular sediments – A. Kudrolli

Context. The ground is constantly shaped by animal and human activities that can further impact the movement of fluids and erosion.[338] Exopedonic and endopedonic activities leading to creation of mounds, voids, and burrows in loose sediments, besides anthropogenic activities leading to desertification, and trawling for resources on the ocean floor are problems of great importance in ecosystem management. To overcome the opacity of granular matter, where much of these activities occur, X-ray imaging and index-matching techniques have been employed to understand locomotion strategies from undulatory to peristaltic motions *in situ*.[339,340] Besides water jets and fluidization, various strategies have been discovered for movements in subsurface materials, from plastic grain rearrangements to sand fluidization and burrow extension by fracture, which vary depending on depth, compaction, and grain size.[341] Considerable work is underway to understand the observed locomotion speeds, and the link to the observed gaits employed, based on the rheology of the medium, as well as in developing models starting from resistive force theory and slender-body theory, which are known in the context of viscously dominated fluid dynamics.[342,343] To understand intruded dynamics in granular media representative of the ground beneath our feet, further work is required to extend rheological models developed under uniform flow and shear conditions to time-dependent and unsteady flows encountered in such dynamics.

Recent advances. These considerations have motivated studies of the drag encountered by spherical and cylindrical solid intruders moving across a granular bed.[344–348] These studies have found that the non-dimensional Inertial Number and Viscous Number used to characterize the properties of granular matter and granular suspensions introduced under uniform shear rate conditions[196,349] can be extended to unsteady cases by using an effective shear rate set by the length scale and speed of the intruder. Visualizations of the flow of the granular medium have revealed that flow is more narrowly confined around the intruder with far greater slip at the solid-medium interface compared with a viscous fluid.[345,348] Granular flow around an intruder was found to result in far greater drag anisotropy compared to viscous flow, which is important for drag-assisted propulsion, with still greater anisotropy while considering grains with negligible surface friction.[347] The experiments robustly support the increase of drag with overburden pressure in a granular bed and scaling of drag with projected cross-sectional area in the case of simple intruder shapes such as spheres and solids. However, wakes generated by more complex or multi-component shapes were found to lead to non-additive drag. In particular, two rods moving in tandem[348] are observed to present a drag as a function of separation distance that is different compared to that in viscous fluids. While drag acting on the leading and trailing rod in viscous fluids at low Reynolds numbers are essentially the same, in a granular material the drag acting on the leading rod exceeds that acting on the trailing rod even in the quasi-static limit.[348] These studies point to the complexity and nuanced nature of granular matter encountered while moving or digging in them.

While the above has focused on the limit where the intruder is strong enough to move the material, a complementary limit is where the intruder cannot move the material, but is restricted to moving within the pore spaces. Thigmotactic behavior, as in motion along the edges of surfaces due to sensory feedback and environmental cues, can play an important role in determining transport.[350] One example is the dynamics of centimeter-scale oligochaeta *Lumbriculus variegatus* in model porous media, where its natural strokes are hindered by the tight passages between idealized grains. A persistent random walk model along boundaries was found to capture the observed time-distributions to escape the dynamical traps posed by the pore-throats.[351] Active polymer models where simple steric interactions are emphasized have a significant role to play in determining general principles of transport in this limit.[352–354] The importance of body shape, stroke, and topology is receiving attention in determining the dynamics of bacteria as also discussed in the following Section 4.2.

Open questions. With the insight obtained through recent studies on the complexity of the granular flow produced by a range of intruders, there is new information to include in constitutive models potentially able to predict the response of the ground also in presence of varying environmental conditions. Tackling the coupling and feedback between the intruder dynamics, including active and adaptive processes, and the ground evolution is the key challenge for the coming years.

to its centrality to construction technologies and the built infrastructure.

Recent advances. Among immediately implementable strategies that would allow for substantial decarbonization of the cement industry, greener cement mixtures based on reduced cement content and partial substitution with clays and natural soils are probably the most interesting and valuable option.[366,367] The soil, the world's oldest construction material, is also probably the most ecologically responsible and a potentially novel source of more sustainable construction technologies. Clay sensitivity to salinity, pH, moisture, and stresses, which are central to cohesive strength, stability of soil and building foundations, originates from the nanoscale physical chemistry and ionic composition of clay layers. From this elemental scale, larger-scale structures with complex pore networks and load bearing properties grow.[138,368] In hydrated clays, nanoscale surface forces develop from the accumulation and confinement of ions in solution between charged surfaces, a phenomenon which also controls the cohesion of hydrated cement and is well-known in soft matter, ranging from colloidal materials to biological systems.[369] However, the cohesive forces that develop during hydration of cement and clays are strongly ion-specific and dramatically depend on confinement and humidity conditions. Hence, they cannot be properly captured by existing mean-field theoretical descriptions used in other cases for surface forces in ionic solutions, raising a number of outstanding fundamental questions on the nanoscale physics of confined ion and water.[364,370,371] Increasing confinement and surface charge densities promote ion–water structures, distinct from bulk ion hydration shells, that become strongly anisotropic, persistent, and self-organized into optimized nearly solid-like assemblies. Under these conditions, the dramatically reduced dielectric screening of water and the highly organized water–ion structures (Fig. 17c) lead to strongly attractive interactions between charged surfaces.

Molecular simulations effectively fill the gap with the experimental characterization of cohesive forces in hydrated clays and cement, providing novel insight into the strong ionic correlations that govern them, to be used in continuum theories and larger scale studies.[364,370,371] The nanoscale forces, in fact, together with the non-equilibrium environmental conditions, eventually determine the growth of microscale grain assemblies, layered meso-phases, and porous structures that can be obtained *via* coarse-grained simulations (Fig. 17d). These forces then also govern the rheology and mechanics of clay-based soil and construction materials, providing the missing link from the nanoscale physical chemistry to the mesoscale aggregation kinetics and morphological variability of soil and clay-based binders.[365,372,373]

Open questions. Understanding how mechanical and rheological behaviors emerge in porous clay matrices that gel and solidify starting from nanoscale forces, which are chemically specific and sensitive to non-equilibrium conditions and environmental reactivity, is an area rich with challenging scientific questions, where soft matter scientists are poised to contribute with key insights. Integrating novel understanding of how and
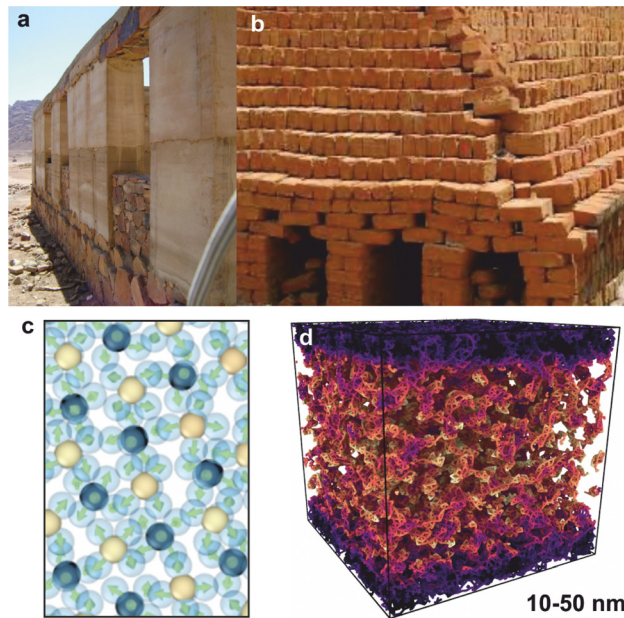

Fig. 17 Earth construction materials, examples, and scientific questions: (a) rammed earth constructions, (b) rural brick kiln, (c) water–ion structures from semiatomistic simulations of Ca ions solutions confined between charged surfaces,[364] and (d) mesoscale porous structures of cement hydrate gels from coarse-grained simulations, where particle sizes are on the order of 10–50 nm.[365]

why cohesive forces emerge in soils into the questions on complex flows, aggregate formation, force chains, and mechanical instabilities at large scales, constitutes one of the challenges for novel research efforts. The opportunities provided by imaging and access to microscopic strains in complex granular assemblies open exciting new research paths.

Discussion

In each contribution associated with one of the four challenges identified in the introduction, a unique research topic, combining soft matter and geosciences, was addressed. The outstanding open questions raised by each author show commonalities that relate to the multi-dimensional, multi-scale, multi-phase, and multi-process character of the ground beneath our feet. Some of the most crucial shared questions are briefly summarized and discussed here.

The opaque and time-dependent nature of the ground profoundly hinders our capacity to observe and understand it. In the laboratory, advancements in microscopic visualization and experimental techniques are, on the one hand, key to remediating this difficulty (see Sections 1.3 and 4.2); yet illuminating all spatial dimensions, while allowing temporal dependencies, is a technical frontier. On the other hand, at the cost of simplifications, properties, stresses, and flow fields in 2D–3D granular porous media can be visualized and quantified (see Sections 1.1, 1.2 and 2.1). In the field, the time-dependent and temporally variable nature of surface and subsurface processes requires additional efforts for monitoring

(see Sections 2.4, 3.3 and 3.5). Extension and advancements in the use of geophysical techniques, such as seismology, hold promise in enabling tracking of the temporal evolution of *e.g.*, transport processes.[224,374] Simultaneously, temporally resolved remote sensing techniques are making details of large-scale phenomena, like ice shelf dynamics, observable (see Sections 2.3 and 3.1).

Though the ground is becoming more observable, seemingly basic questions of when grains start moving, where particles jam, or where and when landslides rupture, are still wide open. Especially in natural systems, identifying the essential conditions (see Sections 1.4 and 1.5), material properties (see Sections 2.1, 2.5 and 4.3), and processes (see Sections 1.1, 2.3 and 2.4) to understand and model the bulk dynamics remains a research frontier. Beyond the relevant components, modeling approaches still struggle to represent key relations (*e.g.*, how microscale processes change the bulk observations, or how to integrate over local conditions or time to obtain bulk mechanical behavior), feedbacks (*e.g.*, how macrostructures affect the microscale conditions, or co-dependent processes and scales[321]), and temporal evolution. While computational advancements enable the modeling of complex systems, coupled dynamics require further efforts in developing the proper way to implement relationships governing elementary phenomena (see Sections 1.5, 3.2, 3.4 and 4.3), including life-related ones (see Sections 1.3, 4.1 and 4.2).

Fundamental open questions, for many of the topics addressed here, emerge from the complex interplay of several phases. The dynamics of, for example, three-phase systems where interfaces of liquid-air-grains evolve over time, are key to a better understanding how natural rafts, such as ice mélanges, behave (see Section 2.3), how debris flows start and stop (see Section 2.2), and how groundwater evaporates into salt crusts (see Section 3.4). Conceptually taming the interactions and feedbacks to understand more than two-phase systems challenges concepts, experiments, and observation throughout the Earth sciences (*e.g.*, ref. 321 and 375–378).

Understanding and modeling contact lines, capillary stresses, and resulting cohesion in particulate materials is a vast and ongoing effort for the case of a single-phase liquid in contact with another fluid and solid particles.[126,379] While, more often than not, flows in the ground are themselves suspensions of minerals (see Sections 1.3 and 1.4), or biological (active) particles (see Sections 4.2 and 4.1), the solid part of the ground itself can be composed of vastly different materials in terms of wettability properties (see Sections 1.4 and 4.2), density (see Sections 1.5 and 2.5), and rigidity (see Section 2.1). Especially where life is involved and shapes its surroundings (see Sections 1.3, 4.1 and 4.2), or where landforms and patterns of different scales interact (see Sections 2.5, 3.4, 3.5 and 3.6), modeling the ground accurately requires solving among the most difficult questions of multi-phases systems.

Another recurrent question for many of the addressed topics is how to model transience in materials state and behavior. The ground is heterogeneous in composition and properties, therefore it presents diverse physicochemical behaviors and properties, such as rigidity (see Section 2.1), plasticity (see Section 1.4), or viscosity (see Section 2.5). As the ground evolves over time under external physicochemical forcings, it also undergoes change in the material bulk dynamics. Such transients may result in instability growth and produce characteristic patterns. In the field these transience dynamics are most often observed indirectly, deduced from the resulting expressions of these dynamics hidden in the ground, like ordered patterns in salt lakes (see Section 3.4), arctic soils (see Section 3.5), ice shelves (see Sections 3.1 and 2.3), or glacial deposits (see Section 3.3). Linking these dynamics to climatic changes, geology, as well as anthropogenic and biogenic activities, poses further outstanding open questions, including topics related to subsurface storage and transport of gases and fluids (see Sections 3.2 and 2.5), or the anticipation of ruptures that can turn into devastating natural hazards (see Sections 1.1 and 2.2).

Conclusion

Most Earth surface materials can be categorized as soft materials. Studying their dynamics necessitates a diversity of approaches, thus understanding the ground is intrinsically a highly interdisciplinary field (Fig. 1). We presented here a soft matter perspective of the "physics of the ground beneath our feet", though diverse, the field contains many commonalities.

As the field is still evolving, it is inhomogeneous and still lacks some common vocabulary; the variations across our subsections reflect that reality. While this perspective brought together many disciplines, we are aware of the inherent limited scope covered, and necessary further linkages to, *e.g.*, the biosphere, atmospheric processes, or transitions from continuum and solid to soft matter. Especially in times of climate changes and resource limitations, gains of fundamental knowledge of the soft matter of the ground will be valuable in our understanding of anthropogenic, climatic, and geophysical hazards.

We are confident that the seeds of ideas presented here will mature as researchers engage with the subject, nucleate new investigations, and help building a percolating framework that supports the field as it grows. We hope for this collective effort to provide a new broad perspective on the field and invite more soft matter scientists to study the fascinating ground on which we live and build our future.

Author contributions

AV and MH contributed equally to this work in leading the manuscript development and writing of the general introduction and discussion sections, in particular. All following authors drafted their sub-section and contributed to the whole manuscript writing, in alphabetical order. Six of the authors contributed equally to this work, in writing their sub-section, and also in overviewing the homogeneity over one entire section; specifically, ICB overviewed Section 1, JCB and KED overviewed Section 2, RG overviewed Section 3, EDG and HAS

overviewed Section 4. All authors were involved in the conceptualization and reviewing the entire article.

Conflicts of interest

There are no conflicts to declare.

Acknowledgements

Notes and references

1 T. Dauxois, T. Peacock, P. Bauer, C. P. Caulfield, C. Cenedese, C. Gorlé, G. Haller, G. N. Ivey, P. F. Linden, E. Meiburg, N. Pinardi, N. M. Vriend and A. W. Woods, *Phys. Rev. Fluids*, 2021, **6**, 020501.

2 R. P. Sharp, *Proc. Natl. Acad. Sci. U. S. A.*, 1982, **79**, 4477–4486.

3 W. E. Dietrich, D. G. Bellugi, L. S. Sklar, J. D. Stock, A. M. Heimsath and J. J. Roering, *Prediction Geomorphology*, 2003, 103–132.

4 M. Houssais and D. J. Jerolmack, *Geomorphology*, 2017, **277**, 251–264.

5 D. J. Jerolmack and K. E. Daniels, *Nat. Rev. Phys.*, 2019, **1**, 716–730.

6 J. K. Jansson and K. S. Hofmockel, *Nat. Rev. Microbiol.*, 2020, **18**, 35–46.

7 S. Doetterl, A. A. Berhe, E. Nadeu, Z. Wang, M. Sommer and P. Fiener, *Earth-Sci. Rev.*, 2016, **154**, 102–122.

8 C.-Y. Lai, J. Kingslake, M. G. Wearing, P.-H. C. Chen, P. Gentine, H. Li, J. J. Spergel and J. M. van Wessem, *Nature*, 2020, **584**, 574–578.

9 A. Singh, G. L. Jackson, M. van der Naald, J. J. de Pablo and H. M. Jaeger, *Phys. Rev. Fluids*, 2022, **7**, 054302.

10 C. G. Sammis and R. L. Biegel, *Pure Appl. Geophys.*, 1989, **131**, 255–271.

11 C. Marone, *Annu. Rev. Earth Planet. Sci.*, 1998, **26**, 643–696.

12 J. R. Rice, *J. Geophys. Res.: Solid Earth*, 2006, **111**, B05311.

13 A. W. Rempel, *Earthquakes: Radiated Energy and the Physics of Faulting*, American Geophysical Union, 2006, pp. 263–270.

14 A. Ruina, *J. Geophys. Res.: Solid Earth*, 1983, **88**, 10359–10370.

15 T. Baumberger and C. Caroli, *Adv. Phys.*, 2006, **55**, 279–348.

16 Q. Li, T. E. Tullis, D. Goldsby and R. W. Carpick, *Nature*, 2011, **480**, 233–236.

17 P. Bhattacharya, A. M. Rubin, E. Bayart, H. M. Savage and C. Marone, *J. Geophys. Res.: Solid Earth*, 2015, **120**, 6365–6385.

18 J.-P. Ampuero and A. M. Rubin, *J. Geophys. Res.: Solid Earth*, 2008, **113**, B01302.

19 B. Ferdowsi and A. M. Rubin, *J. Geophys. Res.: Solid Earth*, 2020, **125**, e2019JB019016.

20 J. R. Rice, N. Lapusta and K. Ranjith, *J. Mech. Phys. Solids*, 2001, **49**, 1865–1898.

21 S. Kim and K. Kamrin, *Phys. Rev. Lett.*, 2020, **125**, 088002.

22 P. Jop, *C. R. Phys.*, 2015, **16**, 62–72.

23 D. L. Henann and K. Kamrin, *Proc. Natl. Acad. Sci. U. S. A.*, 2013, **110**, 6730–6735.

24 Y. Forterre and O. Pouliquen, *Annu. Rev. Fluid Mech.*, 2008, **40**, 1–24.

25 G. Lois, A. Lemaître and J. M. Carlson, *Phys. Rev. E: Stat., Nonlinear, Soft Matter Phys.*, 2005, **72**, 051303.

26 L. E. Silbert, D. Ertas, G. S. Grest, T. C. Halsey, D. Levine and S. J. Plimpton, *Phys. Rev. E: Stat., Nonlinear, Soft Matter Phys.*, 2001, **64**, 051302.

27 P. A. Thompson and G. S. Grest, *Phys. Rev. Lett.*, 1991, **67**, 1751.

28 W. Li, Y. Meng, B. K. Primkulov and R. Juanes, *Phys. Rev. Appl.*, 2021, **16**, 024043.

29 A. Abed Zadeh, J. Barés, T. A. Brzinski, K. E. Daniels, J. Dijksman, N. Docquier, H. O. Everitt, J. E. Kollmer, O. Lantsoght, D. Wang, M. Workamp, Y. Zhao and H. Zheng, *Granular Matter*, 2019, **21**, 83.

30 K. E. Daniels, J. E. Kollmer and J. G. Puckett, *Rev. Sci. Instrum.*, 2017, **88**, 051808.

31 T. S. Majmudar and R. P. Behringer, *Nature*, 2005, **435**, 1079–1082.

32 M. A. Biot, *J. Appl. Phys.*, 1941, **12**, 155–164.

33 R. Juanes, Y. Meng and B. K. Primkulov, *Phys. Rev. Fluids*, 2020, **5**, 110516.

34 K. Terzaghi, *Erdbaumechanik auf Bodenphysikalischer Grundlage*, F. Deuticke, 1925.

35 K. Terzaghi, *Theoretical Soil Mechanics*, John Wiley & Sons, Ltd, 1943, pp. 265–296.

36 M. M. Frocht, *Photoelasticity*, John Wiley & Sons, 1941.

37 J. Palmer, *Nature*, 2017, **548**, 384–386.

38 A. Skarke, C. Ruppel, M. Kodis, D. Brothers and E. Lobecker, *Nat. Geosci.*, 2014, **7**, 657.

39 Y. Guglielmi, F. Cappa, J.-P. Avouac, P. Henry and D. Elsworth, *Science*, 2015, **348**, 1224–1226.

40 M. M. Frocht and R. Guernsey, *A special investigation to develop a general method for three-dimensional photoelastic stress analysis*, National Advisory Committee for Aeronautics technical report, 1952.

41 W. Li and R. Juanes, *Proc. Natl. Acad. Sci. U. S. A.*, 2024, **121**, e2319160121.

42 N. R. Morrow and G. Mason, *Curr. Opin. Colloid Interface Sci.*, 2001, **6**, 321–337.

43 C. C. Mattax and J. Kyte, *Soc. Pet. Eng. J.*, 1962, **2**, 177–184.

44 K. Li and R. N. Horne, *SPE Journal*, 2001, **6**, 375–384.

45 C. Nicolaides, B. Jha, L. Cueto-Felgueroso and R. Juanes, *Water Resour. Res.*, 2015, **51**, 2634–2647.

46 D. B. Bennion and S. Bachu, *SPE Reservoir Eval. Eng.*, 2008, **11**, 487–496.

47 D. B. Bennion and S. Bachu, SPE Annual Technical Conference and Exhibition, 2010.

48 C. U. Hatiboglu and T. Babadagli, *Phys. Rev. E: Stat., Nonlinear, Soft Matter Phys.*, 2008, **77**, 066311.

49 M. A. Celia, S. Bachu, J. Nordbotten and K. Bandilla, *Water Resour. Res.*, 2015, **51**, 6846–6892.

50 C. Schaefer, D. DiCarlo and M. Blunt, *Water Resour. Res.*, 2000, **36**, 885–890.

51 A. Esposito and S. M. Benson, *Energy Procedia*, 2011, **4**, 3216–3223.

52 H. Penvern, M. Zhou, B. Maillet, D. Courtier-Murias, M. Scheel, J. Perrin, T. Weitkamp, S. Bardet, S. Caré and P. Coussot, *Phys. Rev. Appl.*, 2020, **14**, 054051.

53 M. Zhou, S. Caré, A. King, D. Courtier-Murias, S. Rodts, G. Gerber, P. Aimedieu, M. Bonnet, M. Bornert and P. Coussot, *Phys. Rev. Res.*, 2019, **1**, 033190.

54 N. Weisbrod, M. R. Niemet and J. S. Selker, *Adv. Water Resour.*, 2002, **25**, 841–855.

55 F. Tesoro, E. Choong and O. Kimbler, *Wood Fiber Sci.*, 2007, **6**, 226–236.

56 R. Hassanein, H. Meyer, A. Carminati, M. Estermann, E. Lehmann and P. Vontobel, *J. Phys. D: Appl. Phys.*, 2006, **39**, 4284.

57 T. Phenrat, H.-J. Kim, F. Fagerlund, T. Illangasekare, R. D. Tilton and G. V. Lowry, *Environ. Sci. Technol.*, 2009, **43**, 5079–5085.

58 X. Zhao, W. Liu, Z. Cai, B. Han, T. Qian and D. Zhao, *Water Res.*, 2016, **100**, 245–266.

59 S. R. Kanel, J.-M. Greneche and H. Choi, *Environ. Sci. Technol.*, 2006, **40**, 2045–2050.

60 J. Schijven, H. De Bruin, S. Hassanizadeh and A. de Roda Husman, *Water Res.*, 2003, **37**, 2186–2194.

61 H. Zhong, G. Liu, Y. Jiang, J. Yang, Y. Liu, X. Yang, Z. Liu and G. Zeng, *Biotechnol. Adv.*, 2017, **35**, 490–504.

62 R. W. Harvey and S. P. Garabedian, *Environ. Sci. Technol.*, 1991, **25**, 178–185.

63 O. Braun, C. Coquery, J. Kieffer, F. Blondel, C. Favero, C. Besset, J. Mesnager, F. Voelker, C. Delorme and D. Matioszek, *Molecules*, 2021, **27**, 42.

64 C. D. V. Nascimento, J. C. A. Mota, Í. V. Nascimento, G. H. da Silva Albuquerque, R. W. Simmons, C. T. dos Santos Dias and M. C. G. Costa, *Geoderma Regional*, 2021, **26**, e00407.

65 S. Bandak, S. A. R. M. Naeini, E. Zeinali and I. Bandak, *Arab. J. Geosci.*, 2021, **14**, 1–10.

66 M. Garbowski, C. S. Brown and D. B. Johnston, *Restor. Ecol.*, 2020, **28**, A13–A23.

67 J. Misiewicz, S. S. Datta, K. Lejcus and D. Marczak, *Materials*, 2022, **15**, 4465.

68 A. Dechesne, G. Wang, G. Gaolez, D. Or and B. F. Smets, *Proc. Natl. Acad. Sci. U. S. A.*, 2010, **107**, 14369–14372.

69 R. D. Souza, A. Ambrosini and L. M. Passaglia, *Genet. Mol. Biol.*, 2015, **38**, 401–419.

70 G. A. Turnbull, J. A. W. Morgan, J. M. Whipps and J. R. Saunders, *FEMS Microbiol. Ecol.*, 2001, **36**, 21–31.

71 M. Watt, J. Kirkegaard and J. Passioura, *Soil Res.*, 2006, **44**, 299–317.

72 O. O. Babalola, *Biotechnol. Lett.*, 2010, **32**, 1559–1570.

73 J. S. Adadevoh, C. A. Ramsburg and R. M. Ford, *Environ. Sci. Technol.*, 2018, **52**, 7289–7295.

74 J. S. T. Adadevoh, S. Triolo, C. A. Ramsburg and R. M. Ford, *Environ. Sci. Technol.*, 2016, **50**, 181–187.

75 R. M. Ford and R. W. Harvey, *Adv. Water Resour.*, 2007, **30**, 1608–1617.

76 M. Wang, R. M. Ford and R. W. Harvey, *Environ. Sci. Technol.*, 2008, **42**, 3556–3562.

77 J.-B. Raina, V. Fernandez, B. Lambert, R. Stocker and J. R. Seymour, *Nat. Rev. Microbiol.*, 2019, **17**, 284–294.

78 A. Anbari, H.-T. Chien, S. S. Datta, W. Deng, D. A. Weitz and J. Fan, *Small*, 2018, **14**, 1703575.

79 J. Bear, *Dynamics of Fluids in Porous Media*, Courier Corporation, 2013.

80 W. E. Galloway and D. K. Hobday, *Terrigenous Clastic Depositional Systems: Applications to Fossil Fuel and Groundwater Resources*, Springer Science & Business Media, 2012.

81 S. Gasda and M. A. Celia, *Adv. Water Resour.*, 2005, **28**, 493–506.

82 H. King, M. Sansone, P. Kortunov, Y. Xu, N. Callen, S. Chhatre, H. Sahoo and A. Buono, *Petrophysics*, 2018, **59**, 35–43.

83 N. B. Lu, C. A. Browne, D. B. Amchin, J. K. Nunes and S. S. Datta, *Phys. Rev. Fluids*, 2019, **4**, 084303.

84 H. S. Rabbani, D. Or, Y. Liu, C.-Y. Lai, N. B. Lu, S. S. Datta, H. A. Stone and N. Shokri, *Proc. Natl. Acad. Sci. U. S. A.*, 2018, **115**, 4833–4838.

85 N. B. Lu, A. A. Pahlavan, C. A. Browne, D. B. Amchin, H. A. Stone and S. S. Datta, *Phys. Rev. Appl.*, 2020, **14**, 054009.

86 N. B. Lu, D. B. Amchin and S. S. Datta, *Phys. Rev. Fluids*, 2021, **6**, 114007.

87 N. Bizmark, J. Schneider, E. de Jong and S. S. Datta, *Polymer Colloids: Formation, Characterization and Applications*, The Royal Society of Chemistry, 2019, pp. 289–321.

88 E. Dressaire and A. Sauret, *Soft Matter*, 2016, **13**, 37–48.

89 M. Sahimi and A. Imdakm, *Phys. Rev. Lett.*, 1991, **66**, 1169.

90 L. J. Zeman and A. L. Zydney, *Microfiltration and ultrafiltration: principles and applications*, Routledge, 2017.

91 J. Linkhorst, T. Beckmann, D. Go, A. J. Kuehne and M. Wessling, *Sci. Rep.*, 2016, **6**, 22376.

92 I. L. Molnar, W. P. Johnson, J. I. Gerhard, C. S. Willson and D. M. O'Carroll, *Water Resour. Res.*, 2015, **51**, 6804–6845.

93 G. Gerber, M. Bensouda, D. A. Weitz and P. Coussot, *Phys. Rev. Lett.*, 2019, **123**, 158005.

94 Y. Kusaka, J. F. Duval and Y. Adachi, *Environ. Sci. Technol.*, 2010, **44**, 9413–9418.

95 Y.-J. Lin, P. He, M. Tavakkoli, N. T. Mathew, Y. Y. Fatt, J. C. Chai, A. Goharzadeh, F. M. Vargas and S. L. Biswal, *Langmuir*, 2016, **32**, 8729–8734.

96 M. Auset and A. A. Keller, *Water Res. Res.*, 2006, **42**, W12S02.

97 H. M. Wyss, D. L. Blair, J. F. Morris, H. A. Stone and D. A. Weitz, *Phys. Rev. E: Stat., Nonlinear, Soft Matter Phys.*, 2006, **74**, 061402.

98 M. R. de Saint Vincent, M. Abkarian and H. Tabuteau, *Soft Matter*, 2016, **12**, 1041–1050.

99 Y.-J. Lin, P. He, M. Tavakkoli, N. T. Mathew, Y. Y. Fatt, J. C. Chai, A. Goharzadeh, F. M. Vargas and S. L. Biswal, *Energy Fuels*, 2017, **31**, 11660–11668.

100 D. C. Mays, O. T. Cannon, A. W. Kanold, K. J. Harris, T. C. Lei and B. Gilbert, *J. Colloid Interface Sci.*, 2011, **363**, 418–424.

101 E. J. Roth, B. Gilbert and D. C. Mays, *Environ. Sci. Technol.*, 2015, **49**, 12263–12270.

102 X. Li, C.-L. Lin, J. D. Miller and W. P. Johnson, *Environ. Sci. Technol.*, 2006, **40**, 3769–3774.

103 G. Gerber, S. Rodts, P. Aimedieu, P. Faure and P. Coussot, *Phys. Rev. Lett.*, 2018, **120**, 148001.

104 N. Bizmark, J. Schneider, R. D. Priestley and S. S. Datta, *Sci. Adv.*, 2020, **6**, eabc2530.

105 J. Schneider, R. D. Priestley and S. S. Datta, *Phys. Rev. Fluids*, 2021, **6**, 014001.

106 C. A. Browne, A. Shih and S. S. Datta, *Small*, 2020, **16**, 1903944.

107 C. A. Browne, A. Shih and S. S. Datta, *J. Fluid Mech.*, 2020, **890**, A2.

108 C. A. Browne and S. S. Datta, *Sci. Adv.*, 2021, **7**, eabj2619.

109 C. A. Browne, R. B. Huang, C. W. Zheng and S. S. Datta, *J. Fluid Mech.*, 2023, **963**, A30.

110 V. C. Ibezim, R. J. Poole and D. J. Dennis, *J. Non-Newtonian Fluid Mech.*, 2021, **296**, 104638.

111 S. S. Datta, A. M. Ardekani, P. E. Arratia, A. N. Beris, I. Bischofberger, G. H. McKinley, J. G. Eggers, J. E. López-Aguilar, S. M. Fielding, A. Frishman, M. D. Graham, J. S. Guasto, S. J. Haward, A. Q. Shen, S. Hormozi, A. Morozov, R. J. Poole, V. Shankar, E. S. G. Shaqfeh, H. Stark, V. Steinberg, G. Subramanian and H. A. Stone, *Phys. Rev. Fluids*, 2022, **7**, 080701.

112 H. J. Cho, N. B. Lu, M. P. Howard, R. A. Adams and S. S. Datta, *Soft Matter*, 2019, **15**, 4689–4702.

113 T. Bhattacharjee, D. B. Amchin, R. Alert, J. A. Ott and S. S. Datta, *eLife*, 2022, **11**, e71226.

114 T. Bhattacharjee, D. B. Amchin, J. A. Ott, F. Kratz and S. S. Datta, *Biophys. J.*, 2021, **120**, 3483–3497.

115 L. Goehring, A. Nakahara, T. Dutta, S. Kitsunezaki and S. Tarafdar, *Desiccation cracks and their patterns: formation and modeling in science and nature*, John Wiley and Sons, Inc, 2015.

116 W. P. Gates, A. Bouazza and G. J. Churchman, *Elements*, 2009, **5**, 105.

117 D. N. Espinoza and J. C. Santamarina, *Int. J. Greenhouse Gas Control*, 2012, **10**, 351–362.

118 H. J. Cho and S. S. Datta, *Phys. Rev. Lett.*, 2019, **123**, 158004.

119 T. Bhattacharjee and S. S. Datta, *Soft Matter*, 2019, **15**, 9920–9930.

120 T. Bhattacharjee and S. S. Datta, *Nat. Commun.*, 2019, **10**, 2075.

121 D. B. Amchin, J. A. Ott, T. Bhattacharjee and S. S. Datta, *PLoS Comput. Biol.*, 2022, **18**, e1010063.

122 R. C. Grabowski, I. G. Droppo and G. Wharton, *Earth-Sci. Rev.*, 2011, **105**, 101–120.

123 M. Kleber, I. C. Bourg, E. K. Coward, C. M. Hansel, S. C. B. Myneni and N. Nunan, *Nat. Rev. Earth Environ.*, 2021, **2**, 402–421.

124 F. J. Carrillo and I. C. Bourg, *Water Resour. Res.*, 2019, **55**, 8096–8121.

125 T. A. Ghezzehei and D. Or, *Soil Sci. Soc. Am. J.*, 2001, **65**, 624–637.

126 E. Koos and N. Willenbacher, *Science*, 2011, **331**, 897–900.

127 T. R. Underwood and I. C. Bourg, *J. Phys. Chem. C*, 2020, **124**, 3702–3714.

128 X. Shen and I. C. Bourg, *J. Colloid Interface Sci.*, 2021, **584**, 610–621.

129 C. Soulaine and H. A. Tchelepi, *Trans. Porous Media*, 2016, **113**, 431–456.

130 M. A. Murad and C. Moyne, *Comput. Geosci.*, 2008, **12**, 47–82.

131 P. Coussot, *Phys. Rev. Lett.*, 1995, **74**, 3971–3974.

132 F. J. Carrillo and I. C. Bourg, *Phys. Rev. E*, 2021, **103**, 063106.

133 D. L. Kurz, E. Secchi, F. J. Carrillo, I. C. Bourg, R. Stocker and J. Jimenez-Martinez, *Proc. Natl. Acad. Sci. U. S. A.*, 2022, **119**, e2122202119.

134 F. J. Carrillo and I. C. Bourg, *Water Res. Res.*, 2021, **57**, e2020WR028734.

135 C. Di Maio, *Geotechnique*, 1996, **46**, 695–707.

136 A. C. Wiseall, R. J. Cuss, C. C. Graham and J. F. Harrington, *Mineral. Mag.*, 2015, **79**, 1335–1342.

137 S. Rocco, A. W. Woods, J. Harrington and S. Norris, *Geophys. Res. Lett.*, 2017, **44**, 751–759.

138 I. C. Bourg and J. B. Ajo-Franklin, *Acc. Chem. Res.*, 2017, **50**, 2067–2074.

139 A. Seiphoori, X.-G. Ma, P. E. Arratia and D. J. Jerolmack, *Proc. Natl. Acad. Sci. U. S. A.*, 2020, **117**, 2275–2281.

140 R. Kaitna, M. C. Palucis, B. Yohannes, K. M. Hill and W. E. Dietrich, *J. Geophys. Res.: Earth Surface*, 2016, **121**, 415–441.

141 K. M. Hill, J. Gaffney, S. Baumgardner, P. Wilcock and C. Paola, *Water Resour. Res.*, 2017, **53**, 923–941.

142 X. Zheng and I. C. Bourg, *NANO*, 2023, **17**, 19211–19223.

143 A. A. Agles and I. C. Bourg, *J. Phys. Chem. B*, 2023, **127**, 1828–1841.

144 J. S. Wettlaufer, *Philosophical Transactions: Mathematical, Physical and Engineering Sciences*, 2019, **377**, pp. 1–17.

145 N. K. Marath and J. S. Wettlaufer, *Soft Matter*, 2020, **16**, 5886–5891.

146 J. Vachier and J. S. Wettlaufer, *Phys. Rev. E*, 2022, **105**, 024601.

147 S. Tyagi, C. Monteux and S. Deville, *Soft Matter*, 2022, **18**, 4178–4188.

148 D. Gerber, L. A. Wilen, F. Poydenot, E. R. Dufresne and R. W. Style, *Proc. Natl. Acad. Sci. U. S. A.*, 2022, **119**, e2200748119.

149 H. Gupta, *Encyclopedia of Solid Earth Geophysics*, Springer Science & Business Media, 2011.

150 D. L. Turcotte and G. Schubert, *Geodynamics*, Cambridge University Press, 2002.

151 D. J. Jerolmack and K. E. Daniels, *Nat. Rev. Phys.*, 2019, **1**, 716–730.

152 N. S. Deshpande, D. J. Furbish, P. E. Arratia and D. J. Jerolmack, *Nat. Commun.*, 2021, **12**, 3909.

153 R. Kostynick, H. Matinpour, S. Pradeep, S. Haber, A. Sauret, E. Meiburg, T. Dunne, P. Arratia and D. Jerolmack, *Proc. Natl. Acad. Sci. U. S. A.*, 2022, **119**, e2209109119.

154 L. Cascini, M. R. Scoppettuolo and E. Babilio, *Landslides*, 2022, 2839–2851.

155 M. Wyart, *Annales De Physique*, 2005, **30**, 1.

156 X. Mao and T. C. Lubensky, *Ann. Rev. Condens. Matter Phys.*, 2018, **9**, 413–433.

157 K. Liu, J. E. Kollmer, K. E. Daniels, J. M. Schwarz and S. Henkes, *Phys. Rev. Lett.*, 2021, **126**, 088002.

158 T. A. Brzinski and K. E. Daniels, *Phys. Rev. Lett.*, 2018, **120**, 218003.

159 C. S. O'Hern, L. E. Silbert, A. J. Liu and S. R. Nagel, *Phys. Rev. E: Stat., Nonlinear, Soft Matter Phys.*, 2003, **68**, 011306.

160 E. Berthier, M. A. Porter and K. E. Daniels, *Proc. Natl. Acad. Sci. U. S. A.*, 2019, **116**, 16742–16749.

161 E. T. Owens and K. E. Daniels, *Soft Matter*, 2013, **9**, 1214–1219.

162 A. Tordesillas, Z. Zhou and R. Batterham, *Mech. Res. Commun.*, 2018, **92**, 137–141.

163 R. M. Iverson, *Rev. Geophys.*, 1997, **35**, 245–296.

164 D. L. Roth, T. H. Doane, J. J. Roering, D. J. Furbish and A. Zettler-Mann, *Proc. Natl. Acad. Sci. U. S. A.*, 2020, **117**, 25335–25343.

165 R. J. Eyles and R. Ho, *J. Tropical Geography*, 1970, **31**, 40–42.

166 R. W. Fleming and A. M. Johnson, *Q. J. Eng. Geol.*, 1975, **8**, 1–29.

167 A.-V. Auzet and B. Ambroise, *Earth Surf. Processes Landforms*, 1996, **21**, 531–542.

168 N. Matsuoka, *Permafrost Periglacial Processes*, 1998, **9**, 121–133.

169 N. S. Deshpande, P. E. Arratia and D. J. Jerolmack, *Geophys. Res. Lett.*, 2023, **50**, e2023GL102938.

170 M. Houssais, C. Maldarelli and J. F. Morris, *Phys. Rev. Fluids*, 2021, **6**, L012301.

171 F. D. Cunez, E. M. Franklin, M. Houssais, P. Arratia and D. J. Jerolmack, *Phys. Rev. Res.*, 2022, **4**, L022055.

172 B. Ferdowsi, C. P. Ortiz and D. J. Jerolmack, *Proc. Natl. Acad. Sci. U. S. A.*, 2018, **115**, 4827–4832.

173 D. J. Furbish, J. J. Roering, T. H. Doane, D. L. Roth, S. G. W. Williams and A. M. Abbott, *Earth Surf. Dyn.*, 2021, **9**, 539–576.

174 D. J. Furbish, S. G. W. Williams, D. L. Roth, T. H. Doane and J. J. Roering, *Earth Surf. Dyn.*, 2021, **9**, 577–613.

175 D. J. Furbish, S. G. W. Williams and T. H. Doane, *Earth Surf. Dyn.*, 2021, **9**, 615–628.

176 D. J. Furbish and T. H. Doane, *Earth Surf. Dyn.*, 2021, **9**, 629–664.

177 R. M. Iverson, 3rd International Conference on Debris-Flow Hazards Mitigation: Mechanics, Prediction, and Assessment, 2003.

178 K. R. Hubbert, P. M. Wohlgemuth, J. L. Beyers, M. G. Narog and R. Gerrard, *Fire Ecology*, 2012, **8**, 143–162.

179 E. J. Gabet, *Earth Surf. Processes Landforms*, 2003, **28**, 1341–1348.

180 P. Alessio, T. Dunne and K. Morell, *J. Geophys. Res.: Earth Surf.*, 2021, **126**, e2021JF006108.

181 P. Shen, L. Zhang, H. Chen and R. Fan, *Geosci. Model Dev.*, 2018, **11**, 2841–2856.

182 S. H. Cannon, E. R. Bigio and E. Mine, *Hydrolog. Processes*, 2001, **15**, 3011–3023.

183 L. Schippa, *Granularity in Materials Science*, IntechOpen, 2018.

184 R. Sosio and G. B. Crosta, *Water Resour. Res.*, 2009, **45**, W03412.

185 J. D. Parsons, K. X. Whipple and A. Simoni, *J. Geology*, 2001, **109**, 427–447.

186 J. Baker, N. Gray and P. Kokelaar, *Int. J. Erosion Control Eng.*, 2016, **9**, 174–178.

187 J. Kean, D. Staley, J. Lancaster, F. Rengers, B. Swanson, J. Coe, J. Hernandez, A. Sigman, K. Allstadt and D. Lindsay, *Geosphere*, 2019, **15**, 1140–1163.

188 D. Larson, *Am. Sci.*, 1993, **81**, 166–177.

189 R. Ettema, *J. Hydraulic Res.*, 1990, **28**, 673–684.

190 A. Herman, *Ann. Glaciol.*, 2013, **54**, 114–120.

191 M. Jutzeler, R. Marsh, R. J. Carey, J. D. White, P. J. Talling and L. Karlstrom, *Nat. Commun.*, 2014, **5**, 1–10.

192 N. J. Mlot, C. A. Tovey and D. L. Hu, *Proc. Natl. Acad. Sci. U. S. A.*, 2011, **108**, 7669–7673.

193 J. C. Burton, J. M. Amundson, R. Cassotto, C.-C. Kuo and M. Dennin, *Proc. Natl. Acad. Sci. U. S. A.*, 2018, **115**, 5105–5110.

194 A. A. Robel, *Nat. Commun.*, 2017, **8**, 1–7.

195 J. M. Amundson and J. Burton, *J. Geophys. Res.: Earth Surf.*, 2018, **123**, 2243–2257.

196 GDRMiDi, *Eur. Phys. J. E: Soft Matter Biol. Phys.*, 2004, **14**, 341–365.

197 T. Murray, M. Nettles, N. Selmes, L. Cathles, J. C. Burton, T. D. James, S. Edwards, I. Martin, T. O'Farrell and R. Aspey, *et al.*, *Science*, 2015, **349**, 305–308.

198 J. M. Amundson, M. Fahnestock, M. Truffer, J. Brown, M. P. Lüthi and R. J. Motyka, *J. Geophys. Res.: Earth Surf.*, 2010, **115**, F1.

199 R. K. Cassotto, J. C. Burton, J. M. Amundson, M. A. Fahnestock and M. Truffer, *Nat. Geosci.*, 2021, **14**, 417–422.

200 F. Engelund and J. Fredsoe, *Hydrology Res.*, 1976, **7**, 293–306.

201 R. F. Luque and R. V. Beek, *J. Hydraulic Res.*, 1976, **14**, 127–144.

202 E. Meyer-Peter and R. Müller, IAHSR 2nd meeting, Stockholm, appendix 2, 1948.

203 M. Wong and G. Parker, *J. Hydraulic Eng.*, 2006, **132**, 1159–1168.

204 A. Shields, *Application of similarity principles and turbulence research to bed-load movement*, California institute of technology technical report, 1936.

205 P. L. Wiberg and J. D. Smith, *Water Resour. Res.*, 1987, **23**, 1471–1480.

206 G. Parker, *J. Fluid Mech.*, 1978, **89**, 127–146.

207 P. R. Wilcock and J. C. Crowe, *J. Hydraulic Eng.*, 2003, **129**, 120–128.

208 C. B. Phillips and D. J. Jerolmack, *Science*, 2016, **352**, 694–697.

209 C. B. Phillips, C. C. Masteller, L. J. Slater, K. B. J. Dunne, S. Francalanci, S. Lanzoni, D. J. Merritts, E. Lajeunesse and D. J. Jerolmack, *Nat. Rev. Earth Environ.*, 2022, **3**, 406–419.

210 F. Metivier, E. Lajeunesse and O. Devauchelle, *Earth Surf. Dyn.*, 2017, **5**, 187–198.

211 E. R. Mueller, J. Pitlick and J. M. Nelson, *Water Resour. Res.*, 2005, **41**, W04006.

212 J. M. Buffington and D. R. Montgomery, *Water Resour. Res.*, 1997, **33**, 1993–2029.

213 I. Reid, L. E. Frostick and J. T. Layman, *Earth Surf. Processes Landforms*, 1985, **10**, 33–44.

214 C. C. Masteller and N. J. Finnegan, *J. Geophys. Res.: Earth Surf.*, 2017, **122**, 274–289.

215 A.-M. Ockelford and H. Haynes, *Earth Surf. Processes Landforms*, 2013, **38**, 717–727.

216 D. Rickenmann and B. McArdell, *Earth Surf. Processes Landforms*, 2007, **32**, 1362–1378.

217 C. C. Masteller, N. J. Finnegan, J. M. Turowski, E. M. Yager and D. Rickenmann, *Geophys. Res. Lett.*, 2019, **46**, 2583–2591.

218 H. Monteith and G. Pender, *Water Resour. Res.*, 2005, **41**, W12401.

219 H. Haynes and G. Pender, *J. Hydraulic Eng.*, 2007, **133**, 343–349.

220 C. C. Masteller and J. P. Johnson, AGU Fall Meeting Abstracts, 2020, pp. EP008-04.

221 J. M. Turowski, E. M. Yager, A. Badoux, D. Rickenmann and P. Molnar, *Earth Surf. Processes Landforms*, 2009, **34**, 1661–1673.

222 E. Deal, J. G. Venditti, S. J. Benavides, R. Bradley, Q. Zhang, K. Kamrin and J. T. Perron, *Nature*, 2023, **613**, 298–302.

223 A. Burtin, N. Hovius, D. T. Milodowski, Y.-G. Chen, Y.-M. Wu, C.-W. Lin, H. Chen, R. Emberson and P.-L. Leu, *J. Geophys. Res.: Earth Surf.*, 2013, **118**, 1956–1974.

224 K. L. Cook and M. Dietze, *Annu. Rev. Earth Planet. Sci.*, 2022, **50**, 183–204.

225 E. Larose, S. Carrière, C. Voisin, P. Bottelin, L. Baillet, P. Guéguen, F. Walter, D. Jongmans, B. Guillier, S. Garambois, F. Gimbert and C. Massey, *J. Appl. Geophys.*, 2015, **116**, 62–74.

226 B. Schmandt, D. Gaeuman, R. Stewart, S. M. Hansen, V. C. Tsai and J. Smith, *Geology*, 2017, **45**, 299–302.

227 D. L. Roth, G. Jin, M. Bezada, A. Titov, C. C. Masteller, B. Tate and M. Siegfried, AGU Fall Meeting Abstracts, 2022, pp. EP33A-01.

228 H. Albert, F. Costa and J. Mart, *Geology*, 2016, **44**, 211–214.

229 L. Passarelli and E. E. Brodsky, *Geophys. J. Int.*, 2012, **188**, 1025–1045.

230 M. Ripepe, M. Pistolesi, D. Coppola, D. Delle Donne, R. Genco, G. Lacanna, M. Laiolo, E. Marchetti, G. Ulivieri and S. Valade, *Sci. Rep.*, 2017, **7**, 1–9.

231 National Academies of Sciences, *Engineering and Medicine, Volcanic Eruptions and Their Repose, Unrest, Precursors, and Timing*, National Academies Press technical report, 2017.

232 R. Stoiber and S. Williams, *J. Geophys. Res.*, 1986, **91**, 12215–12231.

233 P. Allard, J. Carbonnelle, N. Métrich, H. Loyer and P. Zettwoog, *Nature*, 1994, **368**, 326–330.

234 K. Kazahaya, H. Shinohara and G. Saito, *Bull. Volcanol.*, 1994, **56**, 207–216.

235 J. L. Palma, E. S. Calder, D. Basualto, S. Blake and D. A. Rothery, *J. Geophys. Res.: Solid Earth*, 2008, **113**, 201.

236 C. Oppenheimer, A. S. Lomakina, P. R. Kyle, N. G. Kingsbury and M. Boichu, *Earth Planet. Sci. Lett.*, 2009, **284**, 392–398.

237 J. Woitischek, A. W. Woods, M. Edmonds, C. Oppenheimer, A. Aiuppa, T. D. Pering, T. Ilanko, R. D'Aleo and E. Garaebiti, *J. Volcanol. Geotherm. Res.*, 2020, **398**, 106869.

238 N. Métrich, A. Bertagnini, P. Landi and M. Rosi, *J. Petrology*, 2001, **42**, 1471–1490.

239 L. Francalanci, S. Tommasini and S. Conticelli, *J. Volcanol. Geotherm. Res.*, 2004, **131**, 179–211.

240 L. Francalanci, G. R. Davies, W. Lustenhouwer, S. Tommasini, P. R. Mason and S. Conticelli, *J. Petrology*, 2005, **46**, 1997–2021.

241 J. Suckale, T. Keller, K. V. Cashman and P.-O. Persson, *Geophys. Res. Lett.*, 2016, **43**, 12–071.

242 Z. Qin and J. Suckale, *J. Geophys. Res.: Solid Earth*, 2020, **125**, e2019JB018549.

243 J. Suckale, J. A. Sethian, J.-D. Yu and L. T. Elkins-Tanton, *J. Geophys. Res.: Planets*, 2012, **117**, E08004.

244 Z. Qin, K. Allison and J. Suckale, *J. Comput. Phys.*, 2020, **401**, 109021.

245 K. R. Schwindinger and A. T. Anderson, *Contrib. Mineral. Petrol.*, 1989, **103**, 187–198.

246 P. E. Wieser, Z. Vukmanovic, R. Kilian, E. Ringe, M. B. Holness, J. Maclennan and M. Edmonds, *Geology*, 2019, **47**, 948–952.

247 G. B. Jeffery, *Proc. R. Soc. B*, 1922, **102**, 161–179.

248 M. H. DiBenedetto and N. T. Ouellette, *J. Fluid Mech.*, 2018, **856**, 850–869.

249 M. H. DiBenedetto, J. R. Koseff and N. T. Ouellette, *Phys. Rev. Fluids*, 2019, **4**, 034301.

250 M. DiBenedetto, Z. Qin and J. Suckale, *Sci. Adv.*, 2020, **6**, eabd4850.

251 D. H. Richter and K. J. Murata, US Geological Survey Professional Paper, 1966, 537-D, D1–D12.

252 A. Fowler, *Proc. R. Soc. A*, 1986, **407**, 147–170.

253 C. Schoof, *Nature*, 2010, **468**, 803–806.

254 C. Schoof and I. Hewitt, *Annu. Rev. Fluid Mech.*, 2013, **45**, 217–239.

255 I. J. Hewitt, C. Schoof and M. A. Werder, *J. Fluid Mech.*, 2012, **702**, 157–187.

256 C. Schoof, *J. Fluid Mech.*, 2007, **573**, 27–55.

257 S. S. Pegler, *J. Fluid Mech.*, 2018, **857**, 648–680.

258 R. Sayag and M. G. Worster, *J. Fluid Mech.*, 2019, **881**, 722–738.

259 B. Rallabandi, Z. Zheng, M. Winton and H. A. Stone, *Phys. Rev. Lett.*, 2017, **118**, 128701.

260 J. Wettlaufer and M. G. Worster, *Annu. Rev. Fluid Mech.*, 2006, **38**, 427–452.

261 D. Vella and J. Wettlaufer, *Phys. Rev. Lett.*, 2007, **98**, 088303.

262 D. Vella and J. Wettlaufer, *J. Geophys. Res.: Oceans*, 2008, **113**, C11011.

263 R. Sayag and M. G. Worster, *Geophys. Res. Lett.*, 2013, **40**, 5877–5881.

264 T. J. Wagner, T. D. James, T. Murray and D. Vella, *Geophys. Res. Lett.*, 2016, **43**, 232A–240A.

265 T. J. Wagner, P. Wadhams, R. Bates, P. Elosegui, A. Stern, D. Vella, E. P. Abrahamsen, A. Crawford and K. W. Nicholls, *Geophys. Res. Lett.*, 2014, **41**, 5522–5529.

266 J. Fannon, A. Fowler and I. Moyles, *Proc. R. Soc. A*, 2017, **473**, 20170220.

267 L. K. Zoet and N. R. Iverson, *Science*, 2020, **368**, 76–78.

268 K. Warburton, D. Hewitt and J. Neufeld, *Proc. R. Soc. A*, 2023, **479**, 20220536.

269 A. W. Rempel, J. Wettlaufer and M. G. Worster, *J. Fluid Mech.*, 2004, **498**, 227–244.

270 C. R. Meyer and I. J. Hewitt, *The Cryosphere*, 2017, **11**, 2799–2813.

271 A. Moure, N. Jones, J. Pawlak, C. Meyer and X. Fu, *Water Res. Res.*, 2023, e2022WR034035.

272 D. I. Benn, C. R. Warren and R. H. Mottram, *Earth-Sci. Rev.*, 2007, **82**, 143–179.

273 J. N. Bassis and S. Jacobs, *Nat. Geosci.*, 2013, **6**, 833–836.

274 T. A. Scambos, C. Hulbe, M. Fahnestock and J. Bohlander, *J. Glaciology*, 2000, **46**, 516–530.

275 J. Weertman, *Symposium on the Hydrology of Glaciers*, Cambridge, 1969, vol. 7–13, pp. 139–145.

276 C. Van der Veen, *Cold Regions Sci. Technol.*, 1998, **27**, 31–47.

277 A. F. Banwell, D. R. MacAyeal and O. V. Sergienko, *Geophys. Res. Lett.*, 2013, **40**, 5872–5876.

278 A. A. Robel and A. F. Banwell, *Geophys. Res. Lett.*, 2019, **46**, 12092–12100.

279 R. M. DeConto and D. Pollard, *Nature*, 2016, **531**, 591–597.

280 C.-Y. Lai, L. A. Stevens, D. L. Chase, T. T. Creyts, M. D. Behn, S. B. Das and H. A. Stone, *Nat. Commun.*, 2021, **12**, 1–10.

281 D. L. Chase, C.-Y. Lai and H. A. Stone, *Phys. Rev. Fluids*, 2021, **6**, 084101.

282 V. C. Tsai and J. R. Rice, *J. Geophys. Res.: Earth Surf.*, 2010, **115**, F03007.

283 A. Luckman, D. Jansen, B. Kulessa, E. King, P. Sammonds and D. Benn, *The Cryosphere*, 2012, **6**, 113–123.

284 D. McGrath, K. Steffen, T. Scambos, H. Rajaram, G. Casassa and J. L. R. Lagos, *Ann. Glaciol.*, 2012, **53**, 10–18.

285 W. R. Buck and C.-Y. Lai, *Geophys. Res. Lett.*, 2021, **48**, e2021GL093110.

286 N. B. Coffey, D. R. MacAyeal, L. Copland, D. R. Mueller, O. V. Sergienko, A. F. Banwell and C.-Y. Lai, *J. Glaciology*, 2022, **68**, 867–878.

287 V. Jules, E. Lajeunesse, O. Devauchelle, A. Guérin, C. Jaupart and P.-Y. Lagrée, *J. Fluid Mech.*, 2021, **917**, A13.

288 K. Maher, *Earth Planet. Sci. Lett.*, 2011, **312**, 48–58.

289 C. J. Harman and M. Kim, *Hydrological Processes*, 2019, **33**, 466–475.

290 J. W. Kirchner, X. Feng and C. Neal, *Nature*, 2000, **403**, 524–527.

291 C. Dessert, B. Dupré, J. Gaillardet, L. M. François and C. J. Allègre, *Chem. Geol.*, 2003, **202**, 257–273.

292 V. Jules, PhD thesis, Université de Paris, 2020.

293 J. W. Kirchner, *Water Resour. Res.*, 2009, **45**, W02429.

294 A. Guérin, O. Devauchelle, V. Robert, T. Kitou, C. Dessert, A. Quiquerez, P. Allemand and E. Lajeunesse, *Geophys. Res. Lett.*, 2019, **46**, 7447–7455.

295 D. J. Furbish, P. K. Haff, J. C. Roseberry and M. W. Schmeeckle, *J. Geophys. Res.: Earth Surf.*, 2012, **117**, F03031.

296 D. Chandler, J. Wadham, G. Lis, T. Cowton, A. Sole, I. Bartholomew, J. Telling, P. Nienow, E. Bagshaw, D. Mair, S. Vinen and A. Hubbard, *Nat. Geosci.*, 2013, **6**, 195–198.

297 M. A. Werder, I. J. Hewitt, C. G. Schoof and G. E. Flowers, *J. Geophys. Res.: Earth Surf.*, 2013, **118**, 2140–2158.

298 J. F. Nye, *J. Glaciology*, 1976, **17**, 181–207.

299 A. Damsgaard, J. Suckale, J. A. Piotrowski, M. Houssais, M. R. Siegfried and H. A. Fricker, *J. Glaciology*, 2017, **63**, 1034–1048.

300 I. J. Hewitt and T. T. Creyts, *Geophys. Res. Lett.*, 2019, **46**, 6673–6680.

301 T. K. Lowenstein and L. A. Hardie, *Sedimentology*, 1985, **32**, 627–644.

302 Y. Dang, L. Xiao, Y. Xu, F. Zhang, J. Huang, J. Wang, J. Zhao, G. Komatsu and Z. Yue, *J. Geophys. Res.: Planets*, 2018, **123**, 1910–1933.

303 F. W. Christiansen, *Science*, 1963, **139**, 607–609.

304 J. C. Dixon, in *Aridic Soils, Patterned Ground, and Desert Pavements*, Springer, Dordrecht, The Netherlands, 2009, DOI: 10.1007/978-1-4020-5719-9_5.

305 J. M. Nield, R. G. Bryant, G. F. Wiggs, J. King, D. S. Thomas, F. D. Eckardt and R. Washington, *Geology*, 2015, **43**, 31.

306 J. Lasser, J. M. Nield and L. Goehring, *Earth System Sci. Data*, 2020, **12**, 2881–2898.

307 S. Lokier, *J. Arid Environ.*, 2012, **79**, 32–47.

308 J. Lasser, M. Ernst and L. Goehring, *J. Fluid Mech.*, 2021, **917**, A14.

309 J. Lasser, J. M. Nield, M. Ernst, V. Karius, G. F. S. Wiggs, M. R. Threadgold, C. Beaume and L. Goehring, *Phys. Rev. X*, 2023, **13**, 011025.

310 D. R. Hewitt, G. G. Peng and J. R. Lister, *J. Fluid Mech.*, 2020, **883**, A37.

311 R. Wooding, *J. Fluid Mech.*, 1960, **9**, 183–192.

312 R. A. Wooding, S. W. Tyler, I. White and P. A. Anderson, *Water Resour. Res.*, 1997, **33**, 1199–1217.

313 J. D. Stevens, J. M. S. Jr., C. T. Simmons and T. Fenstemaker, *J. Hydrology*, 2009, **375**, 394–409.

314 D. Groeneveld, J. Huntington and D. Barz, *J. Hydrology*, 2010, **392**, 211–218.

315 H. Eloukabi, N. Sghaier, S. B. Nasrallah and M. Prat, *Int. J. Heat Mass Transfer*, 2013, **56**, 80–93.

316 P. K. Haff, The Scientific Nature of Geomorphology: Proceedings of the 27th Binghamton Symposium in Geomorphology, 1996, p. 337.

317 N. Matsuoka, *Earth-Sci. Rev.*, 2001, **55**, 107–134.

318 H. E. Huppert, *Nature*, 1982, **300**, 427–429.

319 R. C. Glade, M. M. Fratkin, M. Pouragha, A. Seiphoori and J. C. Rowland, *Proc. Natl. Acad. Sci. U. S. A.*, 2021, **118**, e2101255118.

320 N. S. Deshpande, D. J. Furbish, P. E. Arratia and D. J. Jerolmack, *Nat. Commun.*, 2021, **12**, 3909.

321 M. Houssais, C. Maldarelli and J. F. Morris, *Phys. Rev. Fluids*, 2021, **6**, L012301.

322 F. Fazelpour, Z. Tang and K. E. Daniels, *Soft Matter*, 2022, **18**, 1435–1442.

323 S. Mandal, M. Nicolas and O. Pouliquen, *Proc. Natl. Acad. Sci. U. S. A.*, 2020, **117**, 8366–8373.

324 C. Harris, M. C. Davies and B. R. Rea, *Earth Surf. Processes Landforms*, 2003, **28**, 1289–1301.

325 M. Harkema, W. Nijland, S. de Jong, T. Kattenborn and J. Eichel, *Geomorphology*, 2023, **433**, 108727.

326 R. A. Bagnold, *The Physics of Blown Sand and Desert Dunes*, Dover Publications Inc, 1941.

327 R. D. Lorenz and J. R. Zimbelman, *Dune Worlds. How Windblown Sand Shapes Planetary Landscapes*, Springer Praxis Books, 2014.

328 I. Livingstone, G. S. S. Wiggs and C. S. Weaver, *Earth-Sci. Rev.*, 2007, **80**, 239–257.

329 C. J. Berte, *Fighting sand encroachment. Lessons from Mauritania*, Food and Agriculture Organisation of the United Nations, Rome, 2010.

330 B. Andreotti, Y. Forterre and O. Pouliquen, *Granular Media: Between Fluid and Solid*, Cambridge University Press, 2013.

331 K. Kroy, G. Sauermann and H. J. Herrmann, *Phys. Rev. Lett.*, 2002, **88**, 054301.

332 F. Charru, B. Andreotti and P. Claudin, *Annu. Rev. Fluid Mech.*, 2013, **45**, 469–493.

333 K. A. Bacik, S. Lovett, C. P. Caulfield and N. M. Vriend, *Phys. Rev. Lett.*, 2020, **124**, 054501.

334 P. A. Jarvis, K. A. Bacik, C. Narteau and N. M. Vriend, *J. Geophys. Res.: Earth Surf.*, 2022, **127**, e2021JF006492.

335 P. A. Jarvis, C. Narteau, O. Rozier and N. M. Vriend, *Earth Surf. Dyn. Discussions*, 2023, **11**, 803–815.

336 K. A. Bacik, C. P. Caulfield and N. M. Vriend, *Phys. Rev. Lett.*, 2021, **127**, 154501.

337 K. A. Bacik, P. Canizares, C. P. Caulfield, M. J. Williams and N. M. Vriend, *Phys. Rev. Fluids*, 2021, **6**, 104308.

338 F. D. Hole, *Geoderma*, 1981, **25**, 75–112.

339 A. Hosoi and D. I. Goldman, *Annu. Rev. Fluid Mech.*, 2015, **47**, 431–453.

340 A. Kudrolli and B. Ramirez, *Proc. Natl. Acad. Sci. U. S. A.*, 2019, **116**, 25569–25574.

341 K. M. Dorgan, C. J. Law and G. W. Rouse, *Proc. R. Soc. B*, 2013, **280**, 20122948.

342 R. Maladen, Y. Ding, C. Li and D. Goldman, *Science*, 2009, **325**, 314–318.

343 D. Hewitt and N. Balmforth, *J. Fluid Mech.*, 2022, **936**, A17.

344 A. Panaitescu, X. Clotet and A. Kudrolli, *Phys. Rev. E*, 2017, **95**, 032901.

345 R. Jewel, A. Panaitescu and A. Kudrolli, *Phys. Rev. Fluids*, 2018, **3**, 084303.

346 B. Allen and A. Kudrolli, *Phys. Rev. E*, 2019, **100**, 022901.

347 A. Pal and A. Kudrolli, *Phys. Rev. Fluids*, 2021, **6**, 124302.

348 B. Chang and A. Kudrolli, *Phys. Rev. E*, 2022, **105**, 034901.

349 F. Boyer, É. Guazzelli and O. Pouliquen, *Phys. Rev. Lett.*, 2011, **107**, 188301.

350 S. Park, P. M. Wolanin, E. A. Yuzbashyan, H. Lin, N. C. Darnton, J. B. Stock, P. Silberzan and R. Austin, *Proc. Natl. Acad. Sci. U. S. A.*, 2003, **100**, 13910–13915.

351 A. Biswas and A. Kudrolli, *Soft Matter*, 2023, **19**, 4376–4384.

352 C. Bechinger, R. Di Leonardo, H. Löwen, C. Reichhardt, G. Volpe and G. Volpe, *Rev. Mod. Phys.*, 2016, **88**, 045006.

353 Z. Mokhtari and A. Zippelius, *Phys. Rev. Lett.*, 2019, **123**, 028001.

354 C. Kurzthaler, S. Mandal, T. Bhattacharjee, H. Lowen, S. Datta and H. Stone, *Nat. Commun.*, 2021, **12**, 7088.

355 J. M. Melillo, S. D. Frey, K. M. DeAngelis, W. J. Werner, M. J. Bernard, F. P. Bowles, G. Pold, M. A. Knorr and A. S. Grandy, *Science*, 2017, **358**, 101–105.

356 S. Doetterl, A. Stevens, J. Six, R. Merckx, K. Van Oost, M. Casanova Pinto, A. Casanova-Katny, C. Munoz, M. Boudin, E. Zagal Venegas and P. Boeckx, *Nat. Geosci.*, 2015, **8**, 780–783.

357 J. Yang, X. Zhang, I. Bourg and H. Stone, *Nat. Commun.*, 2021, **12**, 622.

358 J. Yang, J. Sanfilippo, N. Abbasi, Z. Gitai, B. Bassler and H. Stone, *Proc. Natl. Acad. Sci. U. S. A.*, 2021, **118**, e2111060118.

359 C. Stanley, G. Grossmann, X. C. I. Solvas and A. DeMello, *Lab Chip*, 2016, **16**, 228–241.

360 K. Aleklett, E. Kiers, P. Ohlsson, T. Shimizu, V. Caldas and E. Hammer, *ISME J.*, 2018, **12**, 312–319.

361 L. Fontaine and R. Auger, *Batir en terre*, Bélin, 2009.

362 H. Guillaud, in *Terra Literature Review. An Overview of Research in Earthen Architecture Conservation*, ed. E. Avrami, H. Guillaud and M. Hardy, The Getty Conservation Institute, Los Angeles, 2009.

363 T. Abergel, B. D. Dean and J. Dulac, *Global Alliance for Buildings and Construction*, 2017.

364 F. Dragulet, A. Goyal, K. Ioannidou, R. J.-M. Pellenq and E. Del Gado, *J. Phys. Chem. B*, 2022, **126**, 4977.

365 A. Goyal, K. Ioannidou, C. Tiede, P. Levitz, R. J.-M. Pellenq and E. Del Gado, *J. Phys. Chem. C*, 2020, **124**, 15500–15510.

366 G. Habert, S. A. Miller, V. M. John, J. L. Provis, A. Favier, A. Horvath and K. L. Scrivener, *Nat. Rev. Earth Environ.*, 2020, **1**, 559–573.

367 A. Gangotra, E. Del Gado and J. I. Lewis, *Commun. Eng.*, 2023, **2**, 6.

368 D. Malakoff, *Science*, 2020, **369**, 894–895.

369 J. N. Israelachvili, *Intermolecular and Surface Forces*, Academic Press, 2015.

370 A. Goyal, I. Palaia, K. Ioannidou, F.-J. Ulm, H. van Damme, R. J.-M. Pellenq, E. Trizac and E. Del Gado, *Sci. Adv.*, 2021, **7**, eabg5882.

371 I. Palaia, A. Goyal, E. Del Gado, L. Samaj and E. Trizac, *J. Phys. Chem. B*, 2022, **126**, 3143.

372 K. Ioannidou, M. Kanduc, L. Li, D. Frenkel, J. Dobnikar and E. Del Gado, *Nat. Commun.*, 2016, **7**, 1–9.

373 K. Ioannidou, K. J. Krakowiak, M. Bauchy, C. G. Hoover, E. Masoero, S. Yip, F.-J. Ulm, P. Levitz, R. J.-M. Pellenq and E. Del Gado, *Proc. Natl. Acad. Sci. U. S. A.*, 2016, **113**, 2029–2034.

374 D. L. Roth, N. J. Finnegan, E. E. Brodsky, D. Rickenmann, J. M. Turowski, A. Badoux and F. Gimbert, *J. Geophys. Res.: Earth Surf.*, 2017, **122**, 1182–1200.

375 S. Lovejoy, H. Gaonac'h and D. Schertzer, *Mathematical Geosciences*, 2008, **40**, 533–573.

376 P. M. Sadler and D. J. Jerolmack, *Geological Society, London, Special Publications*, 2015, **404**, 69–88.

377 R. Hébert, U. Herzschuh and T. Laepple, *Nat. Geosci.*, 2022, **15**, 899–905.

378 C. L. Franzke, S. Barbosa, R. Blender, H. B. Fredriksen, T. Laepple, F. Lambert, T. Nilsen, K. Rypdal, M. Rypdal, M. G. Scotto, S. Vannitsem, N. W. Watkins, L. Yang and N. Yuan, *Rev. Geophys.*, 2020, **58**, e2019RG000657.

379 J. Ha and H.-Y. Kim, *Annu. Rev. Fluid Mech.*, 2020, **52**, 263–284.